Planar Kolmogorov systems coming from spatial Lotka-Volterra systems

Érika Diz-Pita[a], Jaume Llibre[b], M. Victoria Otero-Espinar[a]

[a]*Departamento de Estatística, Análise Matemática e Optimización, Universidade de Santiago de Compostela, 15782 Santiago de Compostela, Spain*
[b]*Departament de Matemàtiques, Universitat Autònoma de Barcelona, 08193 Bellaterra, Barcelona, Spain*

Abstract

In this paper we classify the phase portraits in the Poincaré disc of all the Kolmogorov systems

$$\dot{y} = y\left(b_0 + b_1 yz + b_2 y + b_3 z\right),$$
$$\dot{z} = z\left(c_0 - \mu(b_1 yz + b_2 y + b_3 z)\right),$$

which depend on six parameters. We prove that these systems have 52 topologically distinct phase portraits in the Poincaré disc. These systems are provided by a general 3-dimensional Lotka–Volterra system with a rational first integral of degree two of the form $H = x^i y^j z^k$, restricted to each surface $H(x, y, z) = h$ varying $h \in \mathbb{R}$, with the additional assumption that they have a Darboux invariant of the form $y^\ell z^m e^{st}$.

Keywords: Kolmogorov system, Lotka–Volterra system, phase portrait, Poincaré disc.

The Lotka-Volterra systems have been used for modelling many natural phenomena, such as the time evolution of conflicting species in biology [4, 5, 9, 21, 22, 31], chemical reactions [18], plasma physics [20], hydrodynamics [8], just as other problems from economical science [15, 16, 32] or social science, as the evolution of the internet users [14].

These systems, which are polynomial differential equations of degree two, were initially proposed, independently, by Alfred J. Lotka in 1925 and Vito Volterra in 1926, both in the context of competing species. Later on Lotka-Volterra systems were generalized and considered in arbitrary dimension, i.e.

$$\dot{x}_i = x_i \left(a_{i0} + \sum_{j=1}^{n} a_{ij} x_j \right), \quad i = 1, ..., n.$$

Consequently the applications of these systems started to multiply. Moreover Kolmogorov in [19] extended the Lotka-Volterra systems as follows

$$\dot{x}_i = x_i P_i(x_1, \ldots, x_n), \quad i = 1, ..., n,$$

where P_i are polynomials of degree at most m. These kind of systems are now known as Kolmogorov systems. They have in particular all the applications of the Lotka-Volterra systems as for instance in the study of the black holes in cosmology, see [1, 7].

Email addresses: erikadiz.pita@usc.es (Érika Diz-Pita), jllibre@mat.uab.cat (Jaume Llibre), mvictoria.otero@usc.es (M. Victoria Otero-Espinar)

The global qualitative dynamics of the Lotka-Volterra systems in dimension two has been completely studied in [30], where all the possible phase portraits on the Poincaré disc have been classified.

There are few results about the global dynamics of the Lotka-Volterra systems in dimension three. Our objective is to study the phase portraits of the 3-dimensional Lotka-Volterra systems

$$\begin{aligned} \dot{x} &= x\,(\,a_0 + a_1x + a_2y + a_3z\,),\\ \dot{y} &= y\,(\,b_0 + b_1x + b_2y + b_3z\,),\\ \dot{z} &= z\,(\,c_0 + c_1x + c_2y + c_3z\,), \end{aligned} \tag{0.1}$$

which have a rational first integral of degree two of the form $x^iy^jz^k$. We have used the Darboux theory of integrability to obtain a characterization of these systems. As a result, we have reduced the initial problem to a problem in dimension two, the study of the global dynamics of two families of Kolmogorov systems. We carried out the study of the first family in [11]. In this paper we focus on the second family, which is

$$\begin{aligned} \dot{y} &= y\,(\,b_0 + b_1yz + b_2y + b_3z\,),\\ \dot{z} &= z\,(\,c_0 + c_1yz + c_2y + c_3z\,). \end{aligned} \tag{0.2}$$

Kolmogorov systems (0.2) depend on eight parameters, and this is a big number in order to classify all their distinct topological phase portraits. Then we require that Kolmogorov systems (0.2) have a Darboux invariant of the form $y^\ell z^m e^{st}$, then these systems are reduced to study the Kolmogorov systems

$$\begin{aligned} \dot{y} &= y\,(b_0 + b_1yz + b_2y + b_3z))\,,\\ \dot{z} &= z\,(c_0 - \mu(b_1yz + b_2y + b_3z))\,, \end{aligned} \tag{0.3}$$

which now depend on six parameters. For these Kolmogorov systems we give the topological classification of all their phase portraits in the Poincaré disc. Roughly speaking the Poincaré disc is the closed unit disc centered at the origin of $\mathbb{R}^2$. Its interior is identified with $\mathbb{R}^2$ and the circle of its boundary is identified with the infinity of $\mathbb{R}^2$. In the plane $\mathbb{R}^2$ we can go or come from the infinity in as many directions as points have the circle. The polynomial differential systems can be extended to the closed Poincaré disc, i.e. they can be extended to infinity and in this way we can study their dynamics in a neighborhood of infinity. This extension is called the Poincaré compactification, for more details see Subsection 1.1.

Thus our main result is the following.

Theorem 0.1. *Kolmogorov systems* (0.3) *have* 52 *topologically distinct phase portraits in the Poincaré disc, given in Figure 1.*

Note that systems (0.3) must have $b_1 \neq 0$, otherwise they will be Lotka-Volterra instead of Kolmogorov systems.

In Section 2 we use the Darboux theory of integrability to reduce the Lotka-Volterra systems (0.1) to the Kolmogorov systems (0.3). In Section 3 we give some properties of the systems obtained. In Section 4 we study the local phase portrait of the finite singular points, and in Sections 5 and 6 we do the same with the infinite singular points, applying the blow up technique. Finally in Section 7 we prove Theorem 0.1.

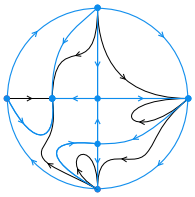

(R1)

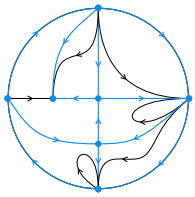

(R2)

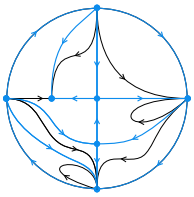

(R3)

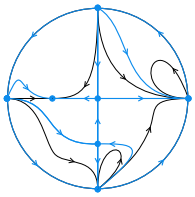

(R4)

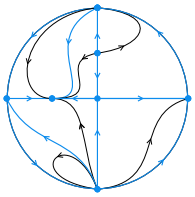

(R5)

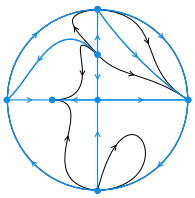

(R6)

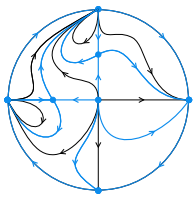

(R7)

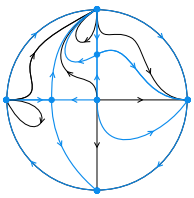

(R8)

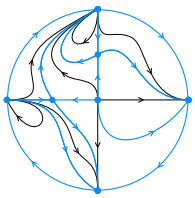

(R9)

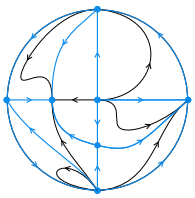

(R10)

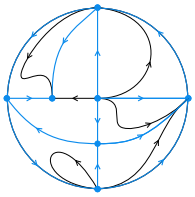

(R11)

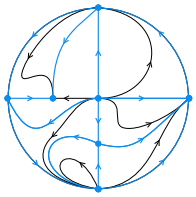

(R12)

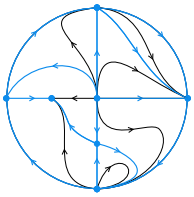

(R13)

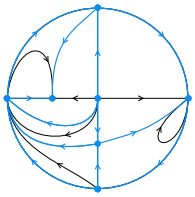

(R14)

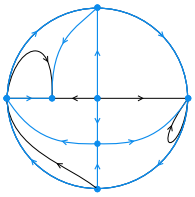

(R15)

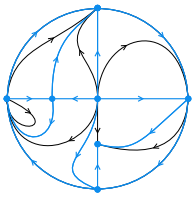

(R16)

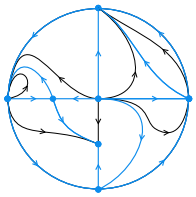

(R17)

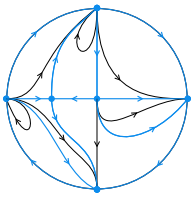

(R18)

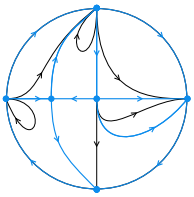

(R19)

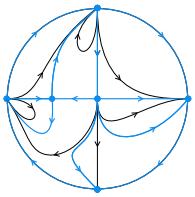

(R20)

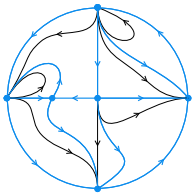

(R21)

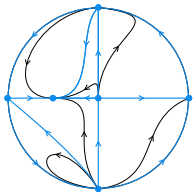

(R22)

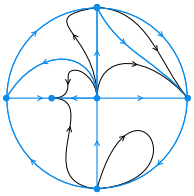

(R23)

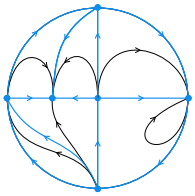

(R24)

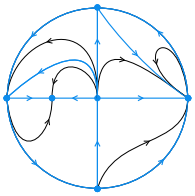

(R25)

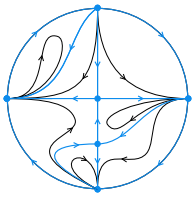

(R26)

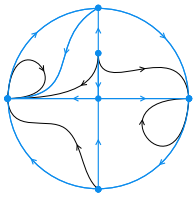

(R27)

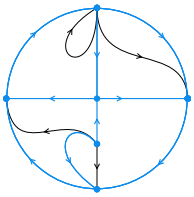

(R28)

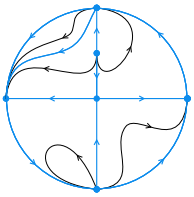

(R29)

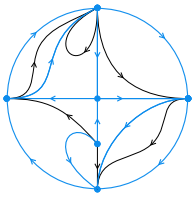

(R30)

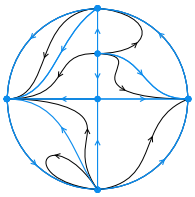

(R31)

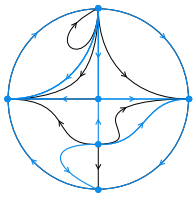

(R32)

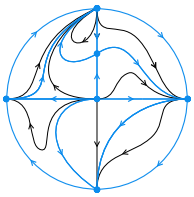

(R33)

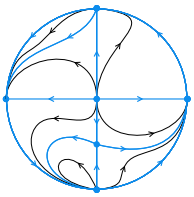

(R34)

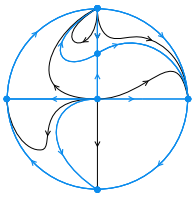

(R35)

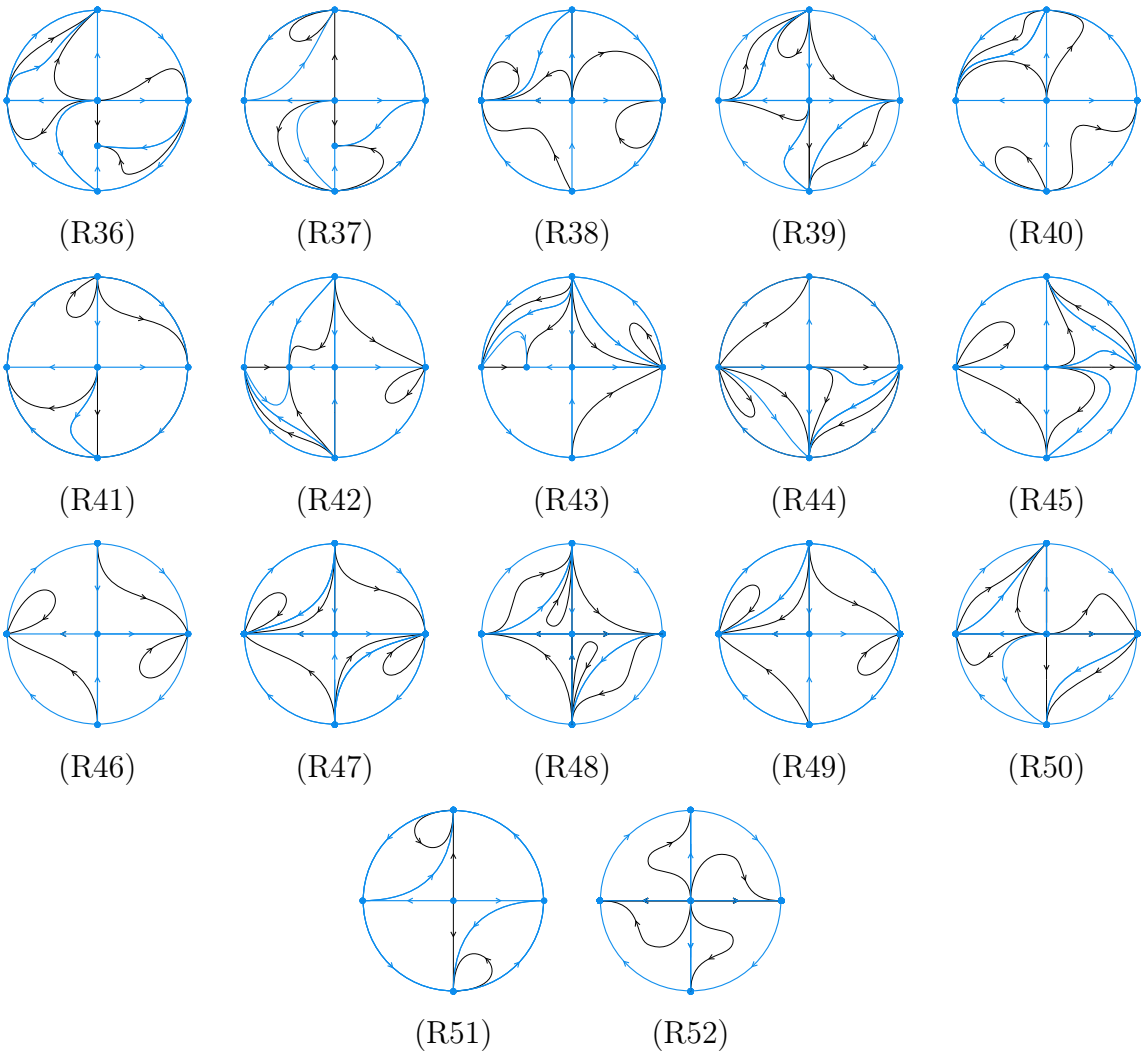

Figure 1: The topologically distinct phase portraits of systems (0.3) in the Poincaré disc.

1. Preliminaries

1.1. Poincaré Compactification

In order to study the behavior of the trajectories of our polynomial differential systems near the infinity we will use the Poincaré compactification. We provide a short summary about this method, more details can be found in [13, Chapter 5].

Let $X = (P(x, w), Q(x, w))$ be a polynomial vector field of degree d defined in $\mathbb{R}^2$. Consider the *Poincaré sphere* $\mathbb{S}^2 = \{w \in \mathbb{R}^3 : w_1^2 + w_2^2 + w_3^2 = 1\}$ and its tangent plane at the point $(0, 0, 1)$ which is identified with $\mathbb{R}^2$.

We consider the central projections $f^+ : \mathbb{R}^2 \to \mathbb{S}^2$ and $f^- : \mathbb{R}^2 \to \mathbb{S}^2$. By definition, $f^+(x)$ is the intersection of the straight line passing through the point x and the origin with the northern hemisphere of $\mathbb{S}^2$, and respectively for $f^-(x)$ with the southern hemisphere. The differential Df^+ and respectively Df^- send the vector field X into a vector field $\overline{X}$ on $\mathbb{S}^2\backslash\mathbb{S}^1$. Note that the points at infinity of $\mathbb{R}^2$ are in bijective correspondence with the points of the equator $\mathbb{S}^1$ of $\mathbb{S}^2$.

The vector field $\overline{X}$ can be extended analytically to a vector field on $\mathbb{S}^2$ multiplying $\overline{X}$ by w_3^d. We denote this vector field by $\rho(X)$, and it is called the *Poincaré compactification* of the vector field X on $\mathbb{R}^2$.

For studying the dynamics of X in the neighborhood of the infinity, we must study the dynamics of $\rho(X)$ near $\mathbb{S}^1$. The sphere $\mathbb{S}^2$ is a 2-dimensional manifold so we need to know the expressions of the vector field $\rho(X)$ in the local charts (U_i, ϕ_i) and (V_i, ψ_i), where $U_i = \{w \in \mathbb{S}^2 : w_i > 0\}$, $V_i = \{w \in \mathbb{S}^2 : w_i < 0\}$, $\phi_i : U_i \longrightarrow \mathbb{R}^2$ and $\psi_i : V_i \longrightarrow \mathbb{R}^2$ for $i = 1, 2, 3$ with $\phi_i(w) = -\psi_i(w) = (w_m/w_i, w_n/w_i)$ for $m < n$ and $m, n \neq i$.

In the local chart (U_1, ϕ_1) the expression of $\rho(X)$ is

$$\dot{u} = v^d \left[-u\, P\left(\frac{1}{v}, \frac{u}{v}\right) + Q\left(\frac{1}{v}, \frac{u}{v}\right)\right],\ \dot{v} = -v^{d+1}\, P\left(\frac{1}{v}, \frac{u}{v}\right). \tag{1.1}$$

In the local chart (U_2, ϕ_2) the expression of $\rho(X)$ is

$$\dot{u} = v^d \left[P\left(\frac{1}{v}, \frac{u}{v}\right) - uQ\left(\frac{1}{v}, \frac{u}{v}\right)\right],\ \dot{v} = -v^{d+1}\, P\left(\frac{1}{v}, \frac{u}{v}\right), \tag{1.2}$$

and in the local chart (U_3, ϕ_3) the expression of $\rho(X)$ is

$$\dot{u} = P(u, v),\ \dot{v} = Q(u, v). \tag{1.3}$$

In the charts (V_i, ψ_i), with $i = 1, 2, 3$, the expression for $\rho(X)$ is the same as in the charts (U_i, ϕ_i) multiplied by $(-1)^{d-1}$.

The equator $\mathbb{S}^1$ is invariant by the vector field $\rho(X)$ and all the singular points of $\rho(X)$ which lie in this equator are called the *infinite singular points* of X. If $w \in \mathbb{S}^1$ is an infinite singular point, then $-w$ is also an infinite singular point and they have the same (respectively opposite) stability if the degree of vector field is odd (respectively even).

The image of the closed northern hemisphere of $\mathbb{S}^2$ onto the plane $w_3 = 0$ under the orthogonal projection π is called the *Poincaré disc* $\mathbb{D}^2$. Since the orbits of $\rho(X)$ on $\mathbb{S}^2$ are symmetric with respect to the origin of $\mathbb{R}^3$, we only need to consider the flow of $\rho(X)$ in the closed northern hemisphere, and we can project the phase portrait of $\rho(X)$ on the northern hemisphere onto the Poincaré disc. We shall present the phase portraits of the polynomial differential systems (0.3) in the Poincaré disc.

1.2. ***Topological equivalence of two polynomial vector fields***

Two polynomial vector fields X_1 and X_2 on $\mathbb{R}^2$ are *topologically equivalent* if there exists a homeomorphism on the Poincaré disc which preserves the infinity $\mathbb{S}^1$ and sends the trajectories of the flow of $\pi(\rho(X_1))$ to the trajectories of the flow of $\pi(\rho(X_2))$, preserving or reversing the orientation of all the orbits.

A *separatrix* of the Poincaré compactification $\pi(\rho(X))$ is an orbit at the infinity $\mathbb{S}^1$, or a finite singular point, or a limit cycle, or an orbit on the boundary of a hyperbolic sector at a finite or an infinite singular point. The set of all separatrices of $\pi(\rho(X))$ is closed and we denote it by Σ_X.

An open connected component of $\mathbb{D}^2 \backslash \Sigma_X$ is a *canonical region* of $\pi(\rho(X))$. The *separatrix configuration* of $\pi(\rho(X))$ is the union of an orbit of each canonical region with the set Σ_X, and it is denoted by $\Sigma_X^{'}$. We denote by S (respectively R) the number of separatrices (respectively canonical regions) of a vector field $\pi(\rho(X))$.

We say that two separatrix configurations $\Sigma_{X_1}^{'}$ and $\Sigma_{X_2}^{'}$ are *topologically equivalent* if there is a homeomorphism $h : \mathbb{D}^2 \to \mathbb{D}^2$ such that $h(\Sigma_{X_1}^{'}) = \Sigma_{X_2}^{'}$.

The following theorem of Markus [27], Neumann [28] and Peixoto [29] allows to investigate only the separatrix configuration of a polynomial differential ssytem in order to determine its phase portrait in the Poincaré disc.

Theorem 1.1. *The phase portraits in the Poincaré disc of two compactified polynomial vector fields $\pi(\rho(X_1))$ and $\pi(\rho(X_2))$ with finitely many separatrices are topologically equivalent if and only if their separatrix configurations Σ'_{X_1} and Σ'_{X_2} are topologically equivalent.*

1.3. ***Blow up technique***

There exist classification theorems for hyperbolic and semi-hyperbolic singular points, and also for nilpotent singular points which can be found in [13, Chapters 2,3]. The centers are more difficult to study, see for instance [13, Chapter 4]. Whereas to study a singular point for which the Jacobian matrix is identically zero, the only possibility is studying each singular point case by case. The main technique to perform the desingularization of a linearly zero singular point is the blow up technique. We give a short summary about this method, more details can be found in [2].

Roughly speaking the idea behind the blow up technique is to explode, through a change of variables that is not a diffeomorphism, the singularity to a line. Then, for studying the original singular point, one studies the new singular points that appear on this line, and this is simpler. If some of these new singular points are linearly zero, the process is repeated. Dumortier proved that this iterative process of desingularization is finite, see [12].

Consider a real planar polynomial differential system of the form

$$\begin{aligned} \dot{x} &= P(x,y) = P_m(x,y) + \dots, \\ \dot{y} &= Q(x,y) = Q_m(x,y) + \dots, \end{aligned} \tag{1.4}$$

where P and Q are coprime polynomials, P_m and Q_m are homogeneous polynomials of degree $m \in \mathbb{N}$ and the dots mean higher order terms in x and y. Note that we are assuming that the origin is a singular point because $m > 0$. We define the *characteristic polynomial* of (1.4) as

$$\mathcal{F}(x,y) := xQ_m(x,y) - yP_m(x,y), \tag{1.5}$$

and we say that the origin is a *nondicritical* singular point if $\mathcal{F} \not\equiv 0$ and a *dicritical* singular point if $\mathcal{F} \equiv 0$. In this last case $P_m = xW_{m-1}$ and $Q_m = yW_{m-1}$, where $W_{m-1} \not\equiv 0$ is a homogeneous polynomial of degree $m-1$. If $y - vx$ is a factor of W_{m-1} and $v = \tan\theta^*$, $\theta^* \in [0, 2\pi)$, then θ^* is a *singular direction*.

The *homogeneous directional blow up in the vertical direction* (resp. in the horizontal direction) is the mapping $(x,y) \to (x,s) = (x, y/x)$ (resp. $(x,y) \to (s,y) = (x/y, y)$), where s is a new variable. This map transforms the origin of (1.4) into the line $x = 0$ (resp. $y = 0$), which is called the *exceptional divisor*. The expression of system (1.4) after the blow up in the vertical direction is

$$\dot{x} = P(x, xs), \quad \dot{s} = \frac{Q(x,xs) - sP(x,xs)}{x}, \tag{1.6}$$

that is always well-defined since we are assuming that the origin is a singularity. After the blow up, we cancel an appearing common factor x^{m-1} (x^m if $\mathcal{F} \equiv 0$). Moreover, the mapping swaps the second and the third quadrants in the vertical directional blow up and the third and the fourth quadrants in the horizontal blow up, which writes as

$$\dot{s} = \frac{P(ys, y) - sQ(ys, y)}{y}, \quad \dot{x} = P(ys, y). \tag{1.7}$$

Propositions 2.1 and 2.2 of [2] provide the relationship between the original singular point of system (1.4) and the new singularities of system (1.6). For additional details see [3].

Finally, to study the behavior of the solutions around the origin of system (1.4), it is necessary to study the singular points of system (1.6) on the exceptional divisor. They correspond to either characteristic directions in the nondicritical case, or singular directions in the dicritical case. It may happen that some of these singular points are linearly zero, in which case we have to repeat the process. As we said before, it is proved in [12] that this chain of blow ups is finite.

1.4. ***Indices of Planar Singular Points***

Given an isolated singularity q of a vector field X, defined on an open subset of $\mathbb{R}^2$ or $\mathbb{S}^2$, we define the index of q by means of the Poincaré Index Formula. We assume that q has the finite sectorial decomposition property. Let E, H and P denote the number of elliptic, hyperbolic and parabolic sectors of q, respectively, and suppose that $E + H + P > 0$. Then the *index of* q is $i_q = (E - H)/2 + 1$, and it is always an integer.

We recall that the Poincaré compactification of a vector field in $\mathbb{R}^2$ introduced in subsection 1.1 is a tangent vector field on the sphere $\mathbb{S}^2$, so the next result will be very useful in our study.

Theorem 1.2 (Poincaré–Hopf Theorem)**.** *For every tangent vector field on $\mathbb{S}^2$ with a finite number of singular points, the sum of their indices is* 2*.*

1.5. ***Invariants and Darboux Theory***

The Darboux Theory of Integrability provides a link between the integrability of polynomial vector fields and the number of invariant algebraic curves that they have. The basic results on dimension two can be found in [13, Chapter 8], and these results have been extended to $\mathbb{R}^n$ and $\mathbb{C}^n$ in [23, 24, 25].

We consider a real polynomial differential system in dimension three, that is a system of the form

$$\begin{aligned} dx/dt = \dot{x} &= P(x, y, z), \\ dy/dt = \dot{y} &= Q(x, y, z), \\ dz/dt = \dot{z} &= R(x, y, z), \end{aligned} \tag{1.8}$$

where P, Q and R are polynomials in the variables x, y and z. We denote by $m = \max\{\deg P, \deg Q, \deg R\}$ the degree of the polynomial system, and we always assume that the polynomials P, Q and R are relatively prime in the ring of the real polynomials in the variables x, y and z.

Theorem 1.3 (Darboux Integrability Theorem)**.** *Suppose that a polynomial system* (1.8) *of degree m admits p irreducible invariant algebraic surfaces $f_i = 0$ with cofactors K_i for $i = 1, \ldots, p$. Then the next statements hold.*

(a) There exist $\lambda_i \in \mathbb{C}$ not all zero such that $\sum_{i=1}^{p} \lambda_i K_i = 0$ if and only if the function $f_1^{\lambda_1} \ldots f_p^{\lambda_p}$ is a first integral of system (1.8)*.*

(b) There exist $\lambda_i \in \mathbb{C}$ not all zero such that $\sum_{i=1}^{p} \lambda_i K_i = -s$ for some $s \in \mathbb{R} \setminus \{0\}$ if and only if the function $f_1^{\lambda_1} \ldots f_p^{\lambda_p} exp(st)$ is a Darboux invariant of system (1.8)*.*

2. Reduction of the Lotka–Volterra systems in $\mathbb{R}^3$ to the Kolmogorov systems (0.3) in $\mathbb{R}^2$

As we said our objective is to study the global dynamics of the Lotka-Volterra systems (0.1) in dimension three, which have a rational first integral of degree two of the form $x^i y^j z^k$. The Darboux theory of integrability allow us to obtain a characterization of these systems.

We consider the irreducible invariant algebraic surfaces $f_1(x,y,z) = x = 0$, $f_2(x,y,z) = y = 0$ and $f_3(x,y,z) = z = 0$ of systems (0.1), with cofactors K_1, K_2 and K_3, respectively. As K_i is the cofactor of f_i we have that

$$Xf_i = P\frac{\partial f_i}{\partial x} + Q\frac{\partial f_i}{\partial y} + R\frac{\partial f_i}{\partial z} = K_i f_i.$$

Then for the invariant algebraic surfaces considered we get the cofactors $K_1 = a_0 + a_1x + a_2y + a_3z$, $K_2 = b_0 + b_1x + b_2y + b_3z$ and $K_3 = c_0 + c_1x + c_2y + c_3z$, respectively.

Applying Theorem 1.3, since we assume that $x^{\lambda_1}y^{\lambda_2}z^{\lambda_3}$ is a first integral of systems (0.1), we get that there exist $\lambda_i \in \mathbb{C}$, with $i \in \{1,2,3\}$, not all zero, such that $\sum_{i=1}^{3} \lambda_i K_i = 0$. Apart from the trivial solution $\{\lambda_1 = 0,\ \lambda_2 = 0,\ \lambda_3 = 0\}$, there are the following three solutions of this equation:

$$S_1 = \{c_0 = 0,\ c_1 = 0,\ c_2 = 0,\ c_3 = 0,\ \lambda_2 = 0,\ \lambda_1 = 0\},$$
$$S_2 = \left\{b_0 = -\frac{c_0\lambda_3}{\lambda_2},\ b_1 = -\frac{c_1\lambda_3}{\lambda_2},\ b_2 = -\frac{c_2\lambda_3}{\lambda_2},\ b_3 = -\frac{c_3\lambda_3}{\lambda_2},\ \lambda_1 = 0\right\}, \text{ and}$$
$$S_3 = \left\{a_0 = \frac{-b_0\lambda_2 - c_0\lambda_3}{\lambda_1},\ a_1 = \frac{-b_1\lambda_2 - c_1\lambda_3}{\lambda_1},\ a_2 = \frac{-b_2\lambda_2 - c_2\lambda_3}{\lambda_1},\ a_3 = \frac{-b_3\lambda_2 - c_3\lambda_3}{\lambda_1}\right\},$$

which give rise to three families of Lotka-Volterra polynomial differential systems of degree two in $\mathbb{R}^3$, with a first integral of the form $x^{\lambda_1}y^{\lambda_2}z^{\lambda_3}$.

If we consider the family given by solution S_1, as the parameters $c_i,\ i = 0, ..., 3$, are zero, we have that $\dot{z} = 0$ and the Lotka-Volterra systems are reduced to:

$$\begin{aligned}
\dot{x} &= x\,(\,a_0 + a_1x + a_2y + a_3z\,),\\
\dot{y} &= y\,(\,b_0 + b_1x + b_2y + b_3z\,),\\
\dot{z} &= 0.
\end{aligned}$$

As $\dot{z} = 0$, z is constant and these systems have $H = z$ as a first integral. Note that if we consider the first integral $H = x^{\lambda_1}y^{\lambda_2}z^{\lambda_3}$, and apply the conditions given by S_1, it is $\lambda_1 = \lambda_2 = 0$, we obtain $H = z^{\lambda_3}$ with $\lambda_3 = 2$, for getting the degree two, but in this case we will consider the simplest first integral. In each invariant plane with z constant, we have Lotka-Volterra polynomial differential systems in $\mathbb{R}^2$. The phase portraits of these systems have been studied in [30], so we are not going to deal with this case.

The topological classification of all the phase portraits in the Poincaré disc of the family given by the solution S_2 has been carried out in [11].

In this paper we study the family given by the solution S_3. This solution provides the values of parameters a_i as a function of the parameters λ_i, b_i and c_i, with $i = 0, .., 3$. Replacing them in the expression of $\dot{x}$ we obtain:

$$\dot{x} = x\left(\frac{-b_0\lambda_2 - c_0\lambda_3}{\lambda_1} + \frac{x\,(-b_1\lambda_2 - c_1\lambda_3)}{\lambda_1} + \frac{y\,(-b_2\lambda_2 - c_2\lambda_3)}{\lambda_1} + \frac{z\,(-b_3\lambda_2 - c_3\lambda_3)}{\lambda_1}\right),$$

and if we denote $\lambda = -\lambda_2/\lambda_1$ and $\mu = -\lambda_3/\lambda_1$, then the original Lotka-Volterra systems become

$$\begin{aligned}
\dot{x} &= x\,(\,b_0\lambda + c_0\mu + x\,(b_1\lambda + c_1\mu) + y\,(b_2\lambda + c_2\mu) + z\,(b_3\lambda + c_3\mu)\,),\\
\dot{y} &= y\,(\,b_0 + b_1x + b_2y + b_3z\,),\\
\dot{z} &= z\,(\,c_0 + c_1x + c_2y + c_3z\,).
\end{aligned}$$

By hypothesis, these systems have the first integral $H = x^{\lambda_1}y^{\lambda_2}z^{\lambda_3}$. Thus, we also can consider as a first integral

$$H = (x^{\lambda_1}y^{\lambda_2}z^{\lambda_3})^{-\frac{1}{\lambda_1}} = x^{-1}\,y^{-\frac{\lambda_2}{\lambda_1}}\,z^{-\frac{\lambda_3}{\lambda_1}} = \frac{y^{\lambda}z^{\mu}}{x}.$$

We want H to be rational of degree two so we must take $\lambda = \mu = 1$. In each level $H = 1/h$, with $h \neq 0$, we will have

$$\frac{1}{h} = \frac{yz}{x} \Longrightarrow x = hyz,$$

and then, for each h, the initial Lotka-Volterra systems on dimension three are reduced to the differential systems on dimension two

$$\begin{aligned}
\dot{y} &= y\,(\,b_0 + b_1hyz + b_2y + b_3z\,),\\
\dot{z} &= z\,(\,c_0 + c_1hyz + c_2y + c_3z\,).
\end{aligned}$$

We must study the phase portraits of this family of differential systems, which is equivalent to study the phase portraits of the following Kolmogorov family on dimension two:

$$\begin{aligned}
\dot{y} &= y\,(\,b_0 + b_1yz + b_2y + b_3z\,),\\
\dot{z} &= z\,(\,c_0 + c_1yz + c_2y + c_3z\,).
\end{aligned} \tag{2.1}$$

In the particular cases in which H is zero or infinity, the differential systems on dimension three are reduced to Lotka-Volterra systems on dimension two, having in each case $z = 0$ and $y = 0$, respectively. We recall that these systems had already been studied in [30].

Systems (2.1) depend on eight parameters and the classification of all their distinct topological phase protraits is huge. For this reason, in the same way that it was done in [11], we study the subclass of them having a Darboux invariant of the form $e^{st}y^{\lambda_1}z^{\lambda_2}$. At first, the expression $\lambda_1K_y + \lambda_2K_z + s$ must be zero by Theorem 1.3(ii), with K_y and K_z the cofactors of the invariant planes $y = 0$ and $z = 0$, respectively. We recall that s and $\lambda_1^2 + \lambda_2^2$ can not be zero.

We obtain the cofactors $K_y = b_0 + b_1yz + b_2y + b_3z$ and $K_z = c_0 + c_1yz + c_2y + c_3z$ and solving the equation $\lambda_1K_x + \lambda_2K_z + s = 0$, we get the following non-trivial solution

$$\left\{c_1 = -\frac{b_1\lambda_1}{\lambda_2},\ \ c_2 = -\frac{b_2\lambda_1}{\lambda_2},\ \ c_3 = -\frac{b_3\lambda_1}{\lambda_2},\ \ s = -b_0\lambda_1 - c_0\lambda_2\right\},$$

which leads to the systems

$$\begin{aligned}
\dot{y} &= y\,(b_0 + b_1yz + b_2y + b_3z)\,,\\
\dot{z} &= z\left(c_0 - \frac{b_1yz\lambda_1}{\lambda_2} - \frac{b_2y\lambda_1}{\lambda_2} - \frac{b_3z\lambda_1}{\lambda_2}\right).
\end{aligned}$$

If we denote $\lambda_2 = \lambda$ and $\lambda_1 = \lambda\mu$, then the systems become

$$\begin{aligned}
\dot{y} &= y\,(b_0 + b_1yz + b_2y + b_3z))\,,\\
\dot{z} &= z\,(c_0 - \mu(b_1yz + b_2y + b_3z))\,,
\end{aligned}$$

and the Darboux invariant is $y^{\lambda\mu}z^{\lambda}e^{-t\lambda(c_0+b_0\mu)}$. But if this is a Daboux invariant, also it is $y^{\mu}ze^{-t(c_0+b_0\mu)}$. Note that in order that we have a Darboux invariant $c_0 + b_0\mu$ cannot be zero.

3. Properties of systems (0.3)

In this section we state some results that will be used on the classification in order to reduce the number of phase portraits appearing. Note that if $b_1 = 0$, then the systems (0.3) are Lotka-Volterra systems in dimension two. A global topological classification of these systems has been completed in [30], so we limit our study to the case $b_1 \neq 0$.

We recall that for obtaining systems (0.3) we have supposed that systems (2.1) have the Darboux invariant $y^\mu z e^{-t(c_0+b_0\mu)}$, so it is required that $c_0 + b_0\mu \neq 0$. The proofs of the next two propositions are easy and we omit them.

Proposition 3.1. *Let $(\tilde{y}(t), \tilde{z}(t))$ be a solution of systems (0.3). In the next cases we obtain other systems with solution $(-\tilde{y}(-t), -\tilde{z}(-t))$.*

1. *If c_0, b_0 and b_1 are not zero, and we change the sign of all of them.*
2. *If $b_0 = 0$ and we change the sign of c_0 and b_1, which are not zero.*
3. *If $c_0 = 0$ and we change the sign of b_0 and b_1, which are not zero.*

Remark 3.2. *By Proposition 3.1 we can limit our study to Kolmogorov systems (0.3) with b_0 non-negative. In the cases with this parameter negative, we will obtain phase portraits symmetric to the ones obtained in the positive cases. And when $b_0 = 0$ we will consider also $c_0 > 0$.*

Proposition 3.3. *Consider systems (0.3) and suppose that $(\tilde{y}(t), \tilde{z}(t))$ is a solution of these systems. If we change b_1 by $-b_1$ and b_2 by $-b_2$ (respectively b_3 by $-b_3$), then $(-\tilde{y}(t), \tilde{z}(t))$ (respectively $(\tilde{y}(t), -\tilde{z}(t))$) is a solution of the obtained systems.*

Corollary 3.4. *Consider systems (0.3) and suppose $(\tilde{y}(t), \tilde{z}(t))$ is a solution. If $b_2 = 0$ (respectively $b_3 = 0$) and we change b_1 by $-b_1$, then $(-\tilde{y}(t), \tilde{z}(t))$ (respectively $(\tilde{y}(t), -\tilde{z}(t))$) is a solution.*

Remark 3.5. *In order to classify all the phase portraits of the Kolmogorov systems (0.3), according with the previous results, it is sufficient to consider $b_2 \geq 0$ and $b_3 \geq 0$. And when $b_2 b_3 = 0$ we will consider also $b_1 > 0$.*

Remark 3.6. *In short according with the previous results and considerations from now on it will be sufficient to study the Kolmogorov systems (0.3) with their parameters satisfying*

$$(H) = \{b_1 \neq 0, c_0 + b_0\mu \neq 0, b_0 \geq 0, b_2 \geq 0, b_3 \geq 0\},$$

and also, if $b_0 = 0$ then $c_0 > 0$ and if $b_2 b_3 = 0$ then $b_1 > 0$.

4. Local study of finite singular points

Systems (0.3) have the following finite singularities:

$$P_0 = (0,0), \quad P_1 = \left(0, \frac{c_0}{\mu b_3}\right) \text{ if } \mu b_3 \neq 0 \text{ and } P_2 = \left(-\frac{b_0}{b_2}, 0\right) \text{ if } b_2 \neq 0.$$

Moreover if $\mu b_3 = 0$ and $c_0 = 0$ all the points on the z-axis are singular points, and if $b_2^2 + b_0^2 = 0$ all the points on the y-axis are singular points, and in both cases the systems

can be reduced to Lotka-Volterra systems in dimension 2. Therefore from now on we will consider the hypothesis

$$(H_1) = \left\{ b_1 \neq 0, b_0\mu + c_0 \neq 0, b_0 \geq 0, b_2 \geq 0, b_3 \geq 0, (\mu b_3)^2 + c_0^2 \neq 0, b_2^2 + b_0^2 \neq 0 \right\}.$$

Assuming (H_1) there are 4 different cases according to the finite singular points existing for systems (0.3), which are given in Table 1. Then we study the possible local phase portraits in each one of the finite singular points under the hypothesis (H_1).

Case	**Conditions**	**Finite singular points**
1	$\mu b_3 \neq 0$, $b_2 \neq 0$.	P_0, P_1, P_2.
2	$\mu b_3 \neq 0$, $b_2 = 0$, $b_0 \neq 0$.	P_0, P_1.
3	$\mu b_3 = 0$, $c_0 \neq 0$, $b_2 \neq 0$.	P_0, P_2.
4	$\mu b_3 = 0$, $c_0 \neq 0$, $b_2 = 0$, $b_0 \neq 0$.	P_0.

Table 1: The different cases for the finite singular points.

The origin is always an isolated singular point for systems (0.3), and we have the next classification for its phase portraits: If $b_0 c_0 \neq 0$ the singularity is hyperbolic and two cases are possible, the origin is a saddle point if $c_0 < 0$, and it is an unstable node if $c_0 > 0$. If $b_0 c_0 = 0$ the origin is a semi-hyperbolic saddle-node.

When P_1 is a singular point of systems (0.3), it can present different phase portraits. If $c_0 \neq 0$ then P_1 is hyperbolic and it can present the following phase portraits: If $c_0\mu(b_0\mu + c_0) > 0$ then P_1 is a saddle, if $c_0 > 0$, $\mu < 0$ and $b_0\mu + c_0 > 0$ it is a stable node, and finally if $c_0 < 0$ and $\mu(b_0\mu + c_0) > 0$ it is an unstable node. The singular point P_1 collides with the origin if $c_0 = 0$.

When P_2 is a singular point of systems (0.3), it is a saddle if $b_0\mu + c_0 > 0$ and it is a stable node if $b_0\mu + c_0 < 0$. If $b_0 = 0$ then P_2 collides with the origin.

Lemma 4.1. *Asumming hypothesis (H_1) there are 22 different cases according to the local phase portrait of the finite singular points of systems (0.3), which are given in Tables 2 - 5.*

Proof. We have to analyse cases 1 to 4 in Table 1 and determine the local phase portraits of the singular points existing in each one of them, according to their individual classification.

We start with the first one, in which the conditions $\mu b_3 \neq 0$ and $b_2 \neq 0$ hold. The singular points are P_0, P_1 and P_2.

Consider case $c_0 < 0$, $b_0 \neq 0$ in which the origin is a saddle. Then P_1 can be a saddle if $\mu(b_0\mu + c_0) < 0$ or an unstable node if $\mu(b_0\mu + c_0) > 0$. If P_1 is a saddle, then P_2 is a stable node, because if it was a saddle with $b_0\mu + c_0 > 0$, then $\mu < 0$ and so $b_0\mu < 0$ and $b_0\mu + c_0 < 0$, which is a contradiction. If P_1 is an unstable node, then P_2 can be either a saddle or a stable node. This leads to cases 1.1 to 1.3 in Table 2.

We continue with the case $c_0 > 0$ and $b_0 > 0$, in which P_0 is an unstable node. Now P_1 can be a saddle or a stable node. If P_1 is a saddle, then P_2 can be a saddle or a stable node, but if P_1 is a stable node then $b_0\mu + c_0 > 0$ and so P_2 is always a saddle. This leads to cases 1.4 to 1.6.

If P_0 is a saddle-node with $c_0 = 0$ and $b_0 > 0$, then P_1 coincides with the origin and P_2 can be a saddle or a stable node. If P_0 is a saddle-node with $b_0 = 0$ and $c_0 > 0$, then P_2 coincides with the origin and P_1 can be a saddle or a stable node. We recall that by the hypothesis it is not possible to have b_0 and c_0 zero simultaneously, b_0 is non negative

and if $b_0 = 0$ then we consider $c_0 > 0$ by Proposition 3.1, so this allow us to conclude the classification in case 1 of Table 1.

Now we study case 2 of Table 1, in which $\mu b_3 \neq 0$, $b_2 = 0$ and $b_0 \neq 0$. The singular points are P_0 and P_1. If P_0 is a saddle, then P_1 can be only a saddle or an unstable node, by the sign of the coefficient c_0. Likewise the sign of c_0 determines that if P_0 is an unstable node, P_1 can be a saddle or a stable node. This leads to cases 2.1 to 2.4 of Table 3. At last, if $c_0 = 0$ then P_1 coincides with the origin and it is a saddle-node.

We address the case 3 of Table 1 in which $\mu b_3 = 0$, $c_0 \neq 0$ and $b_2 \neq 0$. The origin can be a saddle or an unstable node and in both cases P_2 can be a saddle or a stable node, as $b_0 \neq 0$. If $b_0 = 0$ then P_2 coincides with the origin and it is a saddle-node.

Finally in case 4 of Table 1 we have the conditions $\mu b_3 = 0$, $c_0 \neq 0$, $b_2 = 0$ and $b_0 \neq 0$. The unique singular point is the origin and as $c_0 b_0$ cannot be zero, it is either a saddle or an unstable node. □

Case 1: $\mu b_3 \neq 0$, $b_2 \neq 0$.

Sub.	**Conditions**	**Classification**
1.1	$b_0 > 0$, $c_0 < 0$, $\mu > 0$, $(b_0\mu + c_0) < 0$.	P_0 saddle, P_1 saddle, P_2 stable node.
1.2	$b_0 > 0$, $c_0 < 0$, $\mu > 0$, $b_0\mu + c_0 > 0$.	P_0 saddle, P_1 unstable node, P_2 saddle.
1.3	$b_0 > 0$, $c_0 < 0$, $\mu < 0$, $b_0\mu + c_0 < 0$.	P_0 saddle, P_1 unstable node, P_2 stable node.
1.4	$b_0 > 0$, $c_0 > 0$, $\mu > 0$, $b_0\mu + c_0 > 0$.	P_0 unstable node, P_1 saddle, P_2 saddle.
1.5	$b_0 > 0$, $c_0 > 0$, $\mu < 0$, $b_0\mu + c_0 < 0$.	P_0 unstable node, P_1 saddle, P_2 stable node.
1.6	$b_0 > 0$, $c_0 > 0$, $\mu < 0$, $b_0\mu + c_0 > 0$.	P_0 unstable node, P_1 stable node, P_2 saddle.
1.7	$c_0 = 0$, $\mu > 0$.	$P_0 \equiv P_1$ saddle-node, P_2 saddle.
1.8	$c_0 = 0$, $b_0 > 0$, $\mu < 0$.	$P_0 \equiv P_1$ saddle-node, P_2 stable node.
1.9	$b_0 = 0$, $\mu > 0$.	$P_0 \equiv P_2$ saddle-node, P_1 saddle.
1.10	$b_0 = 0$, $c_0 > 0$, $\mu < 0$.	$P_0 \equiv P_2$ saddle-node, P_1 stable node.

Table 2: Classification in case 1 of Table 1 according with the local phase portraits of finite singular points.

Case 2: $\mu b_3 \neq 0$, $b_2 = 0$, $b_0 \neq 0$.

Sub.	**Conditions**	**Classification**
2.1	$b_0 > 0$, $c_0 < 0$, $\mu > 0$, $b_0\mu + c_0 < 0$.	P_0 saddle, P_1 saddle.
2.2	$b_0 > 0$, $c_0 < 0$, $\mu(b_0\mu + c_0) > 0$.	P_0 saddle, P_1 unstable node.
2.3	$b_0 > 0$, $c_0 > 0$, $\mu(b_0\mu + c_0) > 0$.	P_0 unstable node, P_1 saddle.
2.4	$b_0 > 0$, $c_0 > 0$, $\mu < 0$, $b_0\mu + c_0 > 0$.	P_0 unstable node, P_1 stable node.
2.5	$c_0 = 0$, $b_0 > 0$.	$P_0 \equiv P_1$ saddle-node.

Table 3: Classification in case 2 of Table 1 according with the local phase portraits of finite singular points.

Case 3: $\mu b_3 = 0$, $c_0 \neq 0$, $b_2 \neq 0$.

Sub.	Conditions	Classification
3.1	$b_0 > 0$, $c_0 < 0$, $\mu > 0$, $b_0\mu + c_0 > 0$.	P_0 saddle, P_2 saddle.
3.2	$b_0 > 0$, $c_0 < 0$, $b_0\mu + c_0 < 0$.	P_0 saddle, P_3 stable node.
3.3	$b_0 > 0$, $c_0 > 0$, $b_0\mu + c_0 > 0$.	P_0 unstable node, P_2 saddle.
3.4	$b_0 > 0$, $c_0 > 0$,$\mu < 0$, $b_0\mu + c_0 < 0$.	P_0 unstable node, P_2 stable node.
3.5	$b_0 = 0$, $c_0 > 0$.	$P_0 \equiv P_3$ saddle-node.

Table 4: Classification in case 3 of Table 1 according with the local phase portraits of finite singular points.

Case 4: $\mu b_3 = 0$, $c_0 \neq 0$, $b_2 = 0$, $b_0 \neq 0$.

Sub.	Conditions	Classification
4.1	$b_0 c_0 < 0$.	P_0 saddle.
4.2	$b_0 > 0$, $c_0 > 0$.	P_0 unstable node.

Table 5: Classification in case 4 of Table 1 according with the local phase portraits of finite singular points.

5. Local study of infinite singular points in the chart U_1

In order to study the behavior of the trajectories of systems (0.3) near infinity we consider its Poincaré compactification. For the moment we assume the same hypothesis (H_1) than in previous sections. From Section 1 it is enough to study the singular points over $v = 0$ in the chart U_1 and the origin of the chart U_2. We will deal with the study of the origin of chart U_2 in Section 6, so now we focus on the chart U_1. According to equation (1.1) we get the compactification in the local chart U_1, where systems (0.3) write

$$\begin{aligned} \dot{u} &= -b_3(\mu+1)u^2v + (c_0 - b_0)uv^2 - b_1(\mu+1)u^2 - b_2(\mu+1)uv, \\ \dot{v} &= -b_3uv^2 - b_0v^3 - b_1uv - b_2v^2. \end{aligned} \tag{5.1}$$

Taking $v = 0$ we get $\dot{u}\,|_{v=0} = -b_1(\mu+1)u^2$ and $\dot{v}\,|_{v=0} = 0$. Therefore if $\mu = -1$ all points at infinity are singular points, and we will not deal with this situation in this paper. In other case, if $\mu \neq -1$, the only singular point is the origin of U_1, which we denote by O_1. As the linear part of systems (5.1) at the origin is identically zero we use the blow up technique to study it, leading to the next result, which is proved in Subsections 5.1 and 5.2.

From now on we include the condition $\mu \neq -1$ in our hypothesis, so we will work under the conditions

$$(H_2) = \left\{ b_1 \neq 0, b_0\mu + c_0 \neq 0, b_0 \geq 0, b_2 \geq 0, b_3 \geq 0, (\mu b_3)^2 + c_0^2 \neq 0, b_2^2 + b_0^2 \neq 0, \mu \neq -1 \right\}.$$

Lemma 5.1. *Asumming hypothesis (H_2) the origin of the chart U_1 is an infinite singular point of systems (0.3), and it has 27 distinct local phase portraits described in Figure 2.*

In the following subsections we prove Lemma 5.1. For systems (5.1) the characteristic polynomial is $\mathcal{F} = b_2\mu uv^2 + b_1\mu u^2 v$, so the origin is a nondicritical singular point if $\mu \neq 0$ and it is dicritical if $\mu = 0$, so we will study this two cases separately.

We introduce the new variable w_1 by means of the variable change $uw_1 = v$, and get the systems

$$\begin{aligned} \dot{u} &= (c_0 - b_0)u^3w_1^2 - b_3(\mu+1)u^3w_1 - b_2(\mu+1)u^2w_1 - b_1(\mu+1)u^2, \\ \dot{w}_1 &= b_3\mu u^2w_1^2 - c_0u^2w_1^3 + b_2\mu uw_1^2 + b_1\mu uw_1. \end{aligned} \tag{5.2}$$

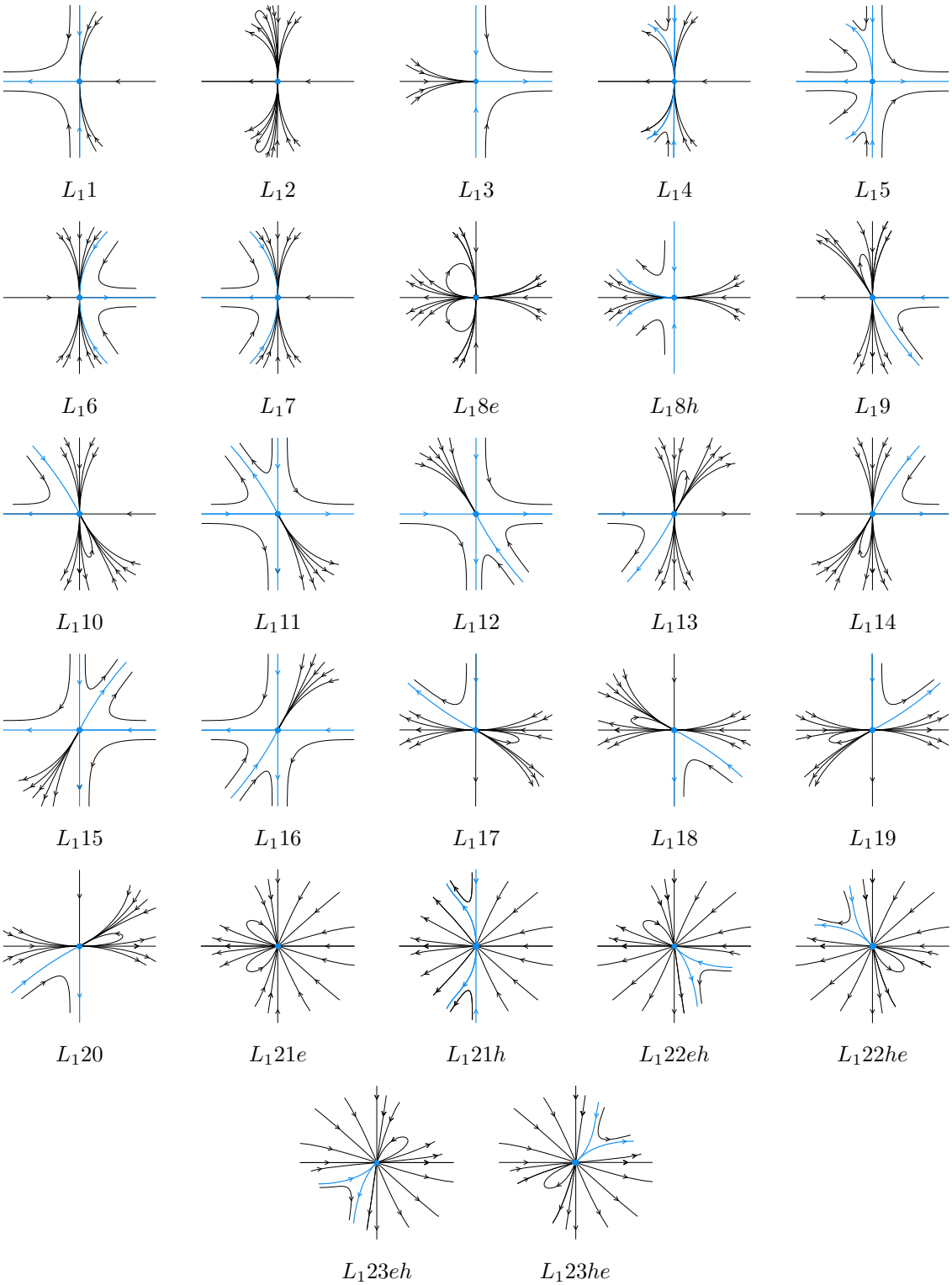

Figure 2: Local phase portraits of the infinite singular point O_1.

In the nondicritical case we have to cancel the common factor u obtaining

$$\begin{aligned} \dot{u} &= (c_0 - b_0)u^2 w_1^2 - b_3(\mu+1)u^2 w_1 - b_2(\mu+1)uw_1 - b_1(\mu+1)u, \\ \dot{w}_1 &= b_3\mu u w_1^2 - c_0 u w_1^3 + b_2\mu w_1^2 + b_1\mu w_1. \end{aligned} \tag{5.3}$$

In the dicritical case, when $\mu = 0$, we must cancel the common factor u^2 and we obtain the systems

$$\begin{aligned} \dot{u} &= (c_0 - b_0)uw_1^2 - b_3 u w_1 - b_2 w_1 - b_1, \\ \dot{w}_1 &= -c_0 w_1^3. \end{aligned} \tag{5.4}$$

5.1. Nondicritical case

At first, it is necessary to study the singular points of systems (5.3) on the exceptional divisor. The origin is always a singular point, and we denote it by Q_0. When $b_2 \neq 0$ there is another singular point, $Q_1 = (0, -b_1/b_2)$.

The origin, Q_0, is always hyperbolic. It is a saddle if $\mu \in (-\infty, -1) \cup (0, +\infty)$, a stable node if $\mu \in (-1, 0)$ and $b_1 > 0$, and an unstable node if $\mu \in (-1, 0)$ and $b_1 < 0$. The singular point Q_1 is always a semi-hyperbolic saddle-node. These conditions come together in the next five subcases.

(A) If $b_2 = 0$, $b_0 \neq 0$ and $\mu \in (-\infty, -1) \cup (0, +\infty)$, then the only singular point on the exceptional divisor is Q_0 which is a saddle. In this case the vertical blow up done does not provide a well determined phase portrait, so it is necessary to apply a horizontal blow up. In order to do that, we introduce the variable $w_1 = u/v$ on systems (5.1) obtaining:

$$\begin{aligned} \dot{w}_1 &= -\mu b_3 v^2 w_1^2 - \mu b_1 v w_1^2 + c_0 v^2 w_1, \\ \dot{v} &= -b_3 v^3 w_1 - b_1 v^2 w_1 - b_0 v^3, \end{aligned} \tag{5.5}$$

and eliminating a common factor v we get the systems

$$\begin{aligned} \dot{w}_1 &= -\mu b_3 v w_1^2 - \mu b_1 w_1^2 + c_0 v w_1, \\ \dot{v} &= -b_3 v^2 w_1 - b_1 v w_1 - b_0 v^2, \end{aligned} \tag{5.6}$$

for which the only singular point on the exceptional divisor is the origin, and it is linearly zero, so we have to repeat the process.

Now the characteristic polynomial is $\mathcal{F} = b_1(\mu - 1)w_1^2 v - (b_0 + c_0)w_1 v^2$, so the origin is always nondicritical. Note that, as $b_1 \neq 0$, $\mathcal{F} \equiv 0$ if and only if $c_0 = -b_0$ and $\mu = 1$, but in that case $b_0\mu + c_0 = 0$ which contradicts hypothesis (H_2). Now we introduce the new variable $w_2 = w_1/v$, obtaining the systems

$$\begin{aligned} \dot{w}_2 &= -b_3(\mu - 1)w_2^2 v^2 - b_1(\mu - 1)w_2^2 v + (b_0 + c_0)w_2 v, \\ \dot{v} &= -b_3 w_2 v^3 - b_1 w_2 v^2 - b_0 v^2, \end{aligned} \tag{5.7}$$

and eliminating a common factor v, we get

$$\begin{aligned} \dot{w}_2 &= -b_3(\mu - 1)w_2^2 v - b_1(\mu - 1)w_2^2 + (b_0 + c_0)w_2, \\ \dot{v} &= -b_3 w_2 v^2 - b_1 w_2 v - b_0 v. \end{aligned} \tag{5.8}$$

The singular points of systems (5.8) on the exceptional divisor are the origin S_0 and the singular point $S_1 = ((b_0 + c_0)/(b_1(\mu - 1)), 0)$ if $\mu \neq 1$ (note that it coincides with the origin in $b_0 + c_0 = 0$). We determine their local phase portraits obtaining the following classification. We start with the cases in which the only singular point on the exceptional divisor is the origin:

(A1) If $b_0 + c_0 = 0$ and $\mu \neq 1$, then the origin is a semi-hyperbolic saddle-node. The relative position and orientation of the hyperbolic and parabolic sectors depends on the sign of μ and $\mu - 1$. Thus we deal with the following subcases.

Subcase (A1.1). Let $\mu > 1$. This determines the sense of the flow on the w_2-axis, so the phase portrait around this axis for systems (5.8) is the one in Figure 3(a).

To return to systems (5.7) we multiply by v, thus the orbits in the third and fourth quadrants change their orientation. Moreover all the points on the w_2-axis become singular points. The resultant phase portrait is given in Figure 3(b).

When going back to the (w_1, v)-plane the third and fourth quadrants swap from the (w_2, v)-plane, and the exceptional divisor shrinks to a point, and hence the orbits are slightly modified. Attending to the expresions of $\dot{w}_1 \mid_{v=0} = -\mu b_1 w_1^2$ and of $\dot{v} \mid_{w_1=0} = -b_0 v^2$, we know the sense of the flow along the axes. Following the results mentioned in Subsection 1.3, we get the phase portrait given in Figure 3(c), and multiplying again by v, the one given in Figure 3(d).

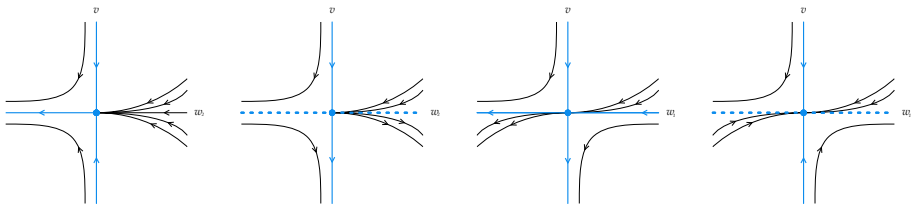

(a) (b) (c) (d)

Figure 3: Desingularization of the origin of systems (5.1) in nondicritical case (A1.1).

Finally we must go back to the (u, v)-plane, swapping again the third and the fourth quadrants and contracting the exceptional divisor to the origin. The orbits tending to the origin in forward or backward time, became orbits tending to the origin in forward or backward time tangent to the v-axis. We get the local phase portrait at the origin for systems (5.1) given in Figure 2($L_1$1).

Subcase (A1.2). Let $\mu \in (0, 1)$. In this case the phase portrait around the w_2-axis for systems (5.8) is the one in Figure 4(a), and multiplying by v, the phase portrait for systems (5.7) is 4(b).

Here, if we try go back to the (w_1, v)-plane, swapping the third and fourth quadrants and shrinking the exceptional divisor, the phase portrait is not determined on the first and third quadrants and around the w_1-axis, and the only information we have is on Figure 4(c). We must do a vertical blow up on system (5.6). We introduce the new variable $w_3 = v/w_1$ and get the system

$$\begin{aligned} \dot{w}_1 &= -b_3 \mu w_1^3 w_3 + c_0 w_1^2 w_3 - \mu b_1 w_1^2, \\ \dot{w}_3 &= b_3(\mu - 1) w_1^2 w_3^2 + b_1(\mu - 1) w_1 w_3. \end{aligned} \tag{5.9}$$

Now we eliminate a common factor w_1:

$$\begin{aligned} \dot{w}_1 &= -b_3 \mu w_1^2 w_3 + c_0 w_1 w_3 - \mu b_1 w_1, \\ \dot{w}_3 &= b_3(\mu - 1) w_1 w_3^2 + b_1(\mu - 1) w_3. \end{aligned} \tag{5.10}$$

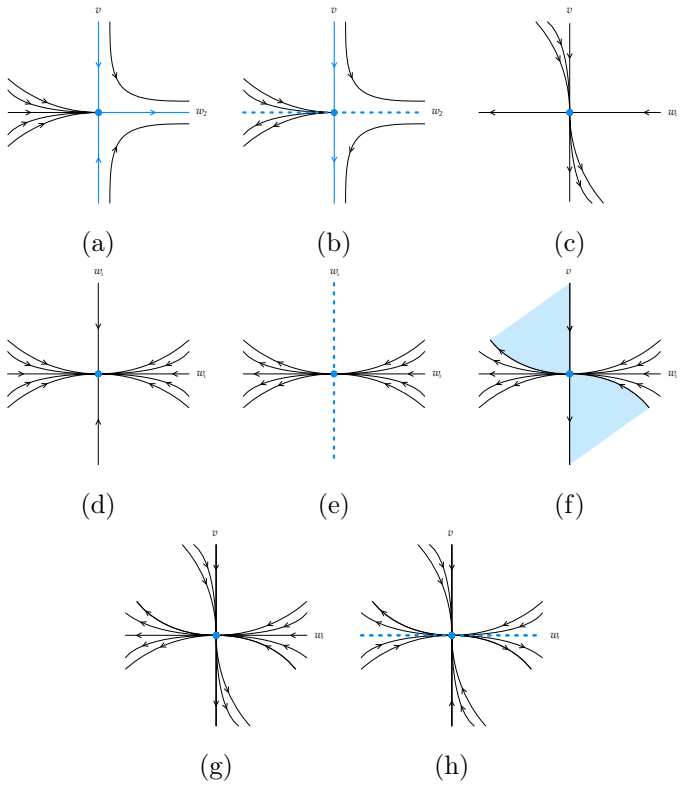

Figure 4: Desingularization of the origin of systems (5.1) in nondicritical case (A1.2).

The only singular point on the exceptional divisor is the origin, which is a stable node. The phase portrait around the w_1-axis for system (5.10) is the one in Figure 4(d), and multiplying by v, the phase portrait for system (5.9) is 4(e). Undoing the vertical blow up we obtain 4(f) where the behaviour around the v-axis, in the coloured regions, is not determined. Combinig this phase portrait with the information on 4(c), it is, that there are orbits which go to the origin tangent to the v-axis on the second quadrant, and there are orbit which leave the origin tangent to the v-axis on the fourth quadrant, we can conclude that for system (5.6) we have phase portrait 4(g). In the second and fourth quadrant it would be possible to have a hyperbolic sector or an elliptic one, but we have proved in the global phase portraits, by applying index theory, that the only feasible option is the one with the elliptic sector.

We must multiply by v and we get the phase portrait given in Figure 3(h) for systems (5.5). Now we undo the first horizontal blow up done and hence we obtain the phase portrait for O_1 given in Figure 2($L_1$2), where the existence of the elliptic sector is proved in the global phase portraits, as we have just mentioned.

Subcase (A1.3). Taking $\mu < 0$ and similarly to the first subcase, we obtain the local phase portait for O_1 given in Figure 2($L_1$3).

(A2) If $\mu = 1$ and $b_0 + c_0 > 0$, then the origin is a saddle. Here, when undoing the blow ups it is necessary again to do a vertical blow up on systems (5.6), and after that we obtain the same phase portrait as in the first subcase, it is $L_1$1.

(A3) If $\mu = 1$ and $b_0 + c_0 < 0$, then the origin is a stable node. Again, including a

vertical blow up on systems (5.6), we obtain phase portait $L_1 2$. As in the first case in which we obtained this local phase portait, the blow up does not determine if the elliptic sectors are indeed elliptic, but we prove it when analyzing the global phase portraits.

Now we consider the cases with two singular points on the exceptional divisor:

(A4) If $b_0 + c_0 > 0$ and $(b_0\mu + c_0)(\mu - 1) < 0$, then the origin and S_1 are saddles. The phase portrait for systems (5.8) is in Figure 5(a) and multiplying by v, the phase portrait for systems (5.7) is in Figure 5(b).

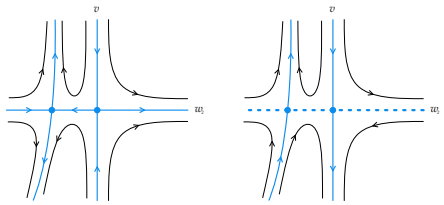

(a) (b)

Figure 5: Desingularization of the origin of systems (5.1) in nondicritical case (A4).

To go back to the (w_1, v)-plane we have to distinguish two cases, one with $\mu < -1$ and other with $\mu \in (0, 1)$. In the first one, the subsequent phase portraits are well determined and we arrive easily to final phase portrait in Figure $2(L_1 5)$. If $\mu \in (0, 1)$, the phase portrait for systems (5.6) is not determined. We must do a vertical blow up, introducing the variable $w_3 = v/w_1$. We get the systems

$$\begin{aligned} \dot{w}_1 &= -b_3\mu w_1^3 w_3 + c_0 w_1^2 w_3 - \mu b_1 w_1^2, \\ \dot{w}_3 &= b_3(\mu - 1)w_1^2 w_3^2 - (b_0 + c_0)w_1 w_3^2 + b_1(\mu - 1)w_1 w_3, \end{aligned} \tag{5.11}$$

and eliminating a common factor w_1:

$$\begin{aligned} \dot{w}_1 &= -b_3\mu w_1^2 w_3 + c_0 w_1 w_3 - \mu b_1 w_1, \\ \dot{w}_3 &= b_3(\mu - 1)w_1 w_3^2 - (b_0 + c_0)w_3^2 + b_1(\mu - 1)w_3. \end{aligned} \tag{5.12}$$

This systems has two singular points on the exceptional divisor: the origin, which is a stable node, and the point $(0, b_1(\mu-1)/(b_0+c_0))$ which is a saddle. Studying the sense of the flow on the axes, we get that the phase portrait for systems (5.12) is the one in Figure 6(a). Multiplying by w_1 and undoing the vertical blow up, we obtain, respectively, the phase portraits on Figure 6(c) and (d). Now the phase portrait for systems (5.6) is well determined, and we can go on undoing the first horizontal blow up, getting the final phase portrait $L_1 4$.

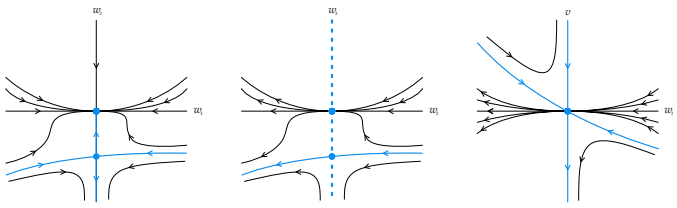

(a) (b) (c)

Figure 6: Vertical blow up on systems (5.6) in nondicritical case (A4).

(A5) If $b_0 + c_0 > 0$ and $(b_0\mu + c_0)(\mu - 1) > 0$, then the origin is a saddle and S_1 is a stable node. We must distinguish three cases in function of the sign of $\mu - 1$, which determines the position of the singular point Q_1 on systems (5.8) and the sense of the flow on the axes on systems (5.6). We do not get any new phase portrait for O_1 in this case. If we take $\mu < 0$ then we obtain the same phase portrait as in subcase A1.3, it is, $L_1 3$, and with $\mu > 1$ we obtain the phase portait $L_1 1$. At last, with $\mu \in (0, 1)$ we obtain the phase portait $L_1 2$, but in this case it is necessary to do a vertical blow up on systems (5.6) during the desingularization process.

(A6) If $b_0 + c_0 < 0$ and $(b_0\mu + c_0)(\mu - 1) > 0$, then the origin is a stable node and S_1 is a saddle. This case is similar to the previous one and we should distinguish three cases: if $\mu < 0$ we obtain the phase portrait $L_1 6$, if $\mu > 1$ we obtain phase portrait $L_1 7$, and if $\mu \in (0, 1)$ we need to do a vertical blow up of systems (5.6) and we obtain phase portait $L_1 2$. As we mentioned before, we have proved that the elliptic sectors are always elliptic in the global phase portraits, although it is not provided by the blow ups.

As in the first case in which we obtained this local phase portait, the blow up does not determine if the elliptic sectors are indeed elliptic, but we prove it when analyzing the global phase portraits.

(A7) If $b_0 + c_0 < 0$ and $(b_0\mu + c_0)(\mu - 1) < 0$, then the origin is a stable node and S_1 is an unstable node and we obtain again phase portrait $L_1 2$.

(B) If $b_2 = 0$, $b_0 \neq 0$ and $\mu \in (-1, 0)$, then Q_0 is a stable node. We obtain phase portraits $L_1 8e$ and $L_1 8h$. Note that the only difference is on the sectors that appear beside the v-axis on the second and third quadrants. On $L_1 8e$ we have elliptic sectors and on $L_1 8h$ we have hyperbolic sectors. It will be enough to apply index theory to know which of them appears in a global phase portait, as we will detail on Section 7.

(C) If $b_2 \neq 0$ and $\mu \in (-\infty, -1) \cup (0, +\infty)$, then Q_0 is a saddle and Q_1 a saddle-node. We must distinguish eight cases. At first, the sign of b_1 determines if singular point Q_1 is on the positive or the negative part of w_1-axis. Also we must fix the signs of μ and $b_0\mu + c_0$ as they determine the position and orientation of the sectors at the saddle-node. The different conditions to study and the corresponding results are the following:

Subcase	**Conditions**	**Phase portrait of O_1**
(C.1)	$b_1 > 0$, $\mu > 0$, $b_0\mu + c_0 < 0$	$L_1 9$
(C.2)	$b_1 > 0$, $\mu > 0$, $b_0\mu + c_0 > 0$	$L_1 10$
(C.3)	$b_1 > 0$, $\mu < -1$, $b_0\mu + c_0 > 0$	$L_1 11$
(C.4)	$b_1 > 0$, $\mu < -1$, $b_0\mu + c_0 < 0$	$L_1 12$
(C.5)	$b_1 < 0$, $\mu > 0$, $b_0\mu + c_0 < 0$	$L_1 13$
(C.6)	$b_1 < 0$, $\mu > 0$, $b_0\mu + c_0 > 0$	$L_1 14$
(C.7)	$b_1 < 0$, $\mu < -1$, $b_0\mu + c_0 > 0$	$L_1 15$
(C.8)	$b_1 < 0$, $\mu < -1$, $b_0\mu + c_0 < 0$	$L_1 16$

In subcases (C.1), (C.2), (C.5) and (C.6), it is necessary to do an horizontal blow up to completely determine the phase portrait of O_1. The process is the same in the four cases so we describe it only for the first one. If we introduce the variable $w_1 = u/v$ in systems (5.1) and we eliminate a common factor v we get

$$\begin{aligned} \dot{w}_1 &= -\mu b_3 w_1^2 v - \mu b_1 w_1^2 - \mu b_2 w_1 + c_0 w_1 v, \\ \dot{v} &= -b_3 w_1 v^2 - b_1 w_1 v - b_0 v^2 - b_2 v. \end{aligned} \tag{5.13}$$

The singular points of systems (5.13) on the exceptional divisor are the origin, which in this case is a stable node, and the point $(-b_2/b_1, 0)$ which is a saddle-node. Thus, attending to the sense of the flow on the axes, the phase portrait of these systems around the w_1-axis is the one in Figure 7(a). Multiplying by w_1 we get the phase portrait on Figure 7(b). Then we undo the horizontal blow up: we swap the third and fourth quadrants, contract the exceptional divisor into the origin and modify the orbits according the results mentioned in Subection 1.3. We recall that, for example, the separatrix of singular point $(-b_2/b_1, 0)$ which is on the third quadrant, goes into a separatrix on the fourth quadrant that starts from the origin with slope $-b_2/b_1$. Now the phase portrait for systems (5.1) is well determined and as we said it is the one on Figure 2($L_1$9).

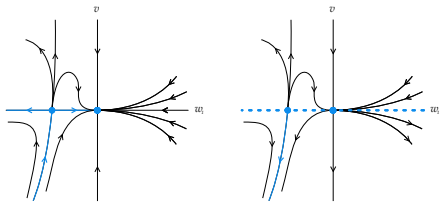

(a) (b)

Figure 7: Horizontal blow up on systems (5.1) in nondicritical case (C.1).

(D) If $b_2 = 0$, $b_0 \neq 0$ and $\mu \in (-\infty, -1) \cup (0, +\infty)$, then Q_0 is a stable node and Q_1 a saddle-node. We separate two cases as the sign of $b_0\mu + c_0$ determines the position of the saddle-node sectors. If $b_0\mu + c_0 > 0$ we obtain phase portait $L_1$17 and if $b_0\mu + c_0 < 0$ then we obtain phase portait $L_1$18.

(E) If $b_2 = 0$, $b_0 \neq 0$ and $\mu \in (-\infty, -1) \cup (0, +\infty)$, then Q_0 is an unstable node and Q_1 a saddle-node. If $b_0\mu > 0$ we obtain phase portait $L_1$19 and if $b_0\mu < 0$ then we obtain phase portait $L_1$20.

5.2. Dicritical case

Now we study the case with $\mu = 0$, i.e, the dicritical case. Systems (5.4) would have a singular point on the exceptional divisor if and only if $c_0 = 0$ and $b_2 \neq 0$, but as we are considering $\mu = 0$, it is not possible because then we would have $b_0\mu + c_0 = 0$ which contradicts hypothesis (H_2). Then there are no singular points on the exceptional divisor.

We must consider four cases depending on whether b_2 is zero or not, and the sign of b_1. If $b_2 = 0$ then the sign of $\dot{u}$ does not change along the w_1-axis, but if $b_2 \neq 0$, $\dot{u}$ changes its sign at the point $(0, -b_1/b_2)$.

If $b_2 = 0$ (then we assume $b_1 > 0$ by Remark 3.6), the flow around the w_1 axis is as represented in Figure 8(a). Multiplying by u^2 all the points on the w_1-axis become singular

points, but the sense of the flow remains the same in all regions, see Figure 8(b). At last, going back to the (u, v)-plane we get that there are orbits which tend to the origin with any slope on quadrants first and fourth, and there are orbits leaving the origin with any slope on quadrant second and third, but also there are sectors which are not determined in this quadrants near the v-axis. This sectors, coloured on Figure 8(c), can be elliptic or hyperbolic, and this can be determined on the global phase portraits by applying index theory, as we will expain on Section 7. As a result we can have phase portraits on Figure 2($L_1 21e$) or ($L_1 21h$).

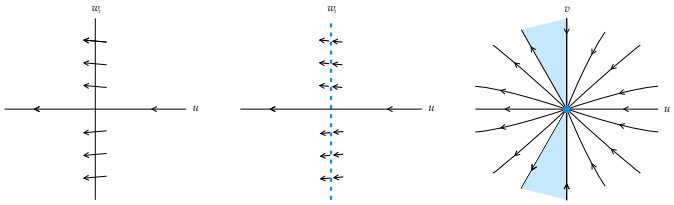

(a) (b) (c)

Figure 8: Desingularization of the origin of systems (5.1) in dicritical case with $b_2 = 0$ and $b_1 > 0$. When the blue sectors instead of be filled with elliptic sectors, are filled with hyperbolic ones, then the boundaries of the blue sectors arrive to the singular point with the same slope.

If $b_2 > 0$ and $b_1 > 0$, the flow on the w_1 axis changes its direction at the point $(0, -b_1/b_2)$, as represented in Figure 9(a). Multiplying by u^2 the sense of the flow does not change but all the points on the w_1-axis become singular points, see Figure 9(b). Going back to the (u, v)-plane there are again two sectors that are not well determined, the ones coloured on Figure 9(c) on quadrants second and fourth, and they can be either hyperbolic or elliptic. In this case, it can be proved by index theory that there are always a hyperbolic sector and an elliptic sector, but their positions change depending on the global phase portrait we are studying. The two possibilities are the ones on Figure 2($L_1 22eh$) and ($L_1 22he$).

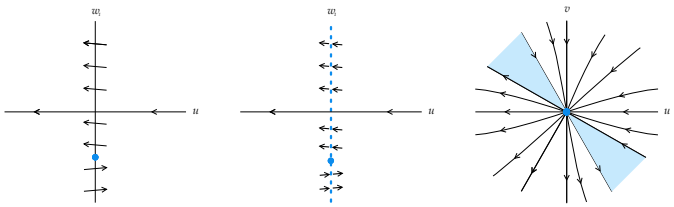

(a) (b) (c)

Figure 9: Desingularization of the origin of systems (5.1) in dicritical case with $b_2 > 0$ and $b_1 > 0$. One of the two blue sectors is elliptic and the other is hyperbolic. The hyperbolic sector must have its two boundaries arriving with the same slope at the singular point.

If $b_2 > 0$ and $b_1 < 0$, similarly to the previous case we obtain phase portraits on Figure 2($L_1 23eh$) or ($L_1 23he$).

We note that in this classification there are local phase portraits which are topologically equivalent, see for example in Figure 2 the phase potraits $L_1 2$, $L_1 8e$ and $L_1 22e$, but we maintain the distinction here as a result of the application of the blow up technique. In the final global classification the phase portraits which are topologically equivalent are unified.

6. Local study of infinite singular points in the chart U_2

According to equation (1.2), we get the compactification in the local chart U_2, where systems (0.3) writes

$$\begin{aligned} \dot{u} &= b_2(\mu+1)u^2v + (b_0-c_0)uv^2 + b_1(\mu+1)u^2 + b_3(\mu+1)uv, \\ \dot{v} &= b_2\mu uv^2 - c_0v^3 + b_1\mu uv + b_3v^2. \end{aligned} \tag{6.1}$$

In the local chart U_2 we only need to study its singularity localized at the origin, denoted by O_2, because its other infinite singularities have already been studied in the local chart U_1. As the linear part of systems (6.1) at the origin is identically zero we must use the blow up technique to study it. We obtain the next result, which is proved below.

Lemma 6.1. *Asumming hypothesis* (H_2) *the origin of the chart* U_2 *is an infinite singular point of systems* (0.3)*, and it has* 26 *distinct local phase portraits described in Figure 10.*

For systems (6.1), the characteristic polynomial is $\mathcal{F} = -b_1u^2v - b_3uv^2 \not\equiv 0$, so the origin is a nondicritical singular point. We introduce the variable w_1 by means of the variable change $uw_1 = v$ and we eliminate a common factor u, then we get the systems

$$\begin{aligned} \dot{u} &= (b_0-c_0)u^2w_1^2 + b_2(\mu+1)u^2w_1 + b_3(\mu+1)uw_1 + b_1(\mu+1)u \\ \dot{w}_1 &= -b_0uw_1^3 - b_2uw_1^2 - b_3w_1^2 - b_1w_1. \end{aligned} \tag{6.2}$$

The singular points on the exceptional divisor $u = 0$ of systems (6.2) are the origin S_0 and the singular point $S_1 = (0, -b_1/b_3)$ if $b_3 \neq 0$. This point S_1 is a semi-hyperbolic saddle-node whenever it exists, while the origin can be a saddle if $\mu > -1$, a stable node if $\mu < -1$ and $b_1 > 0$ and an unstable node if $\mu < -1$ and $b_1 < 0$. Then we must study five different subcases originated by these conditions.

(a) If $b_3 = 0$, $c_0 \neq 0$ and $\mu > -1$, then S_0 is a saddle. Note that once we fix $b_3 = 0$ we can assume $b_1 > 0$ by Remark 3.6. In this case the vertical blow up done does not provide a well determined phase portrait, so we must proceed similarly to the case (A) in Section 5, doing an horizontal blow up. In order to do that, we introduce the variable $w_1 = u/v$ on systems (6.1) and eliminate a common factor v obtaining:

$$\begin{aligned} \dot{w}_1 &= b_2w_1^2v + b_1w_1^2 + b_0w_1v, \\ \dot{v} &= b_2\mu w_1v^2 + b_1\mu w_1v - c_0v^2, \end{aligned} \tag{6.3}$$

for which the only singular point on the exceptional divisor is the origin, and it is linearly zero, so we have to repeat the process. The characteristic polynomial is $\mathcal{F} = b_1(\mu-1)w_1^2v - (b_0+c_0)w_1v^2$, so the origin is always nondicritical by the same reasoning as in (A). Now we introduce the new variable $w_2 = w_1/v$, obtaining the system

$$\begin{aligned} \dot{w}_2 &= b_2(1-\mu)w_2^2v^2 + b_1(1-\mu)w_2^2v + (b_0+c_0)w_2v, \\ \dot{v} &= b_2\mu w_2v^3 + b_1\mu w_2v^2 - c_0v^2, \end{aligned} \tag{6.4}$$

and eliminating a common factor v, we get

$$\begin{aligned} \dot{w}_2 &= b_2(1-\mu)w_2^2v + b_1(1-\mu)w_2^2 + (b_0+c_0)w_2, \\ \dot{v} &= b_2\mu w_2v^2 + b_1\mu w_2v - c_0v. \end{aligned} \tag{6.5}$$

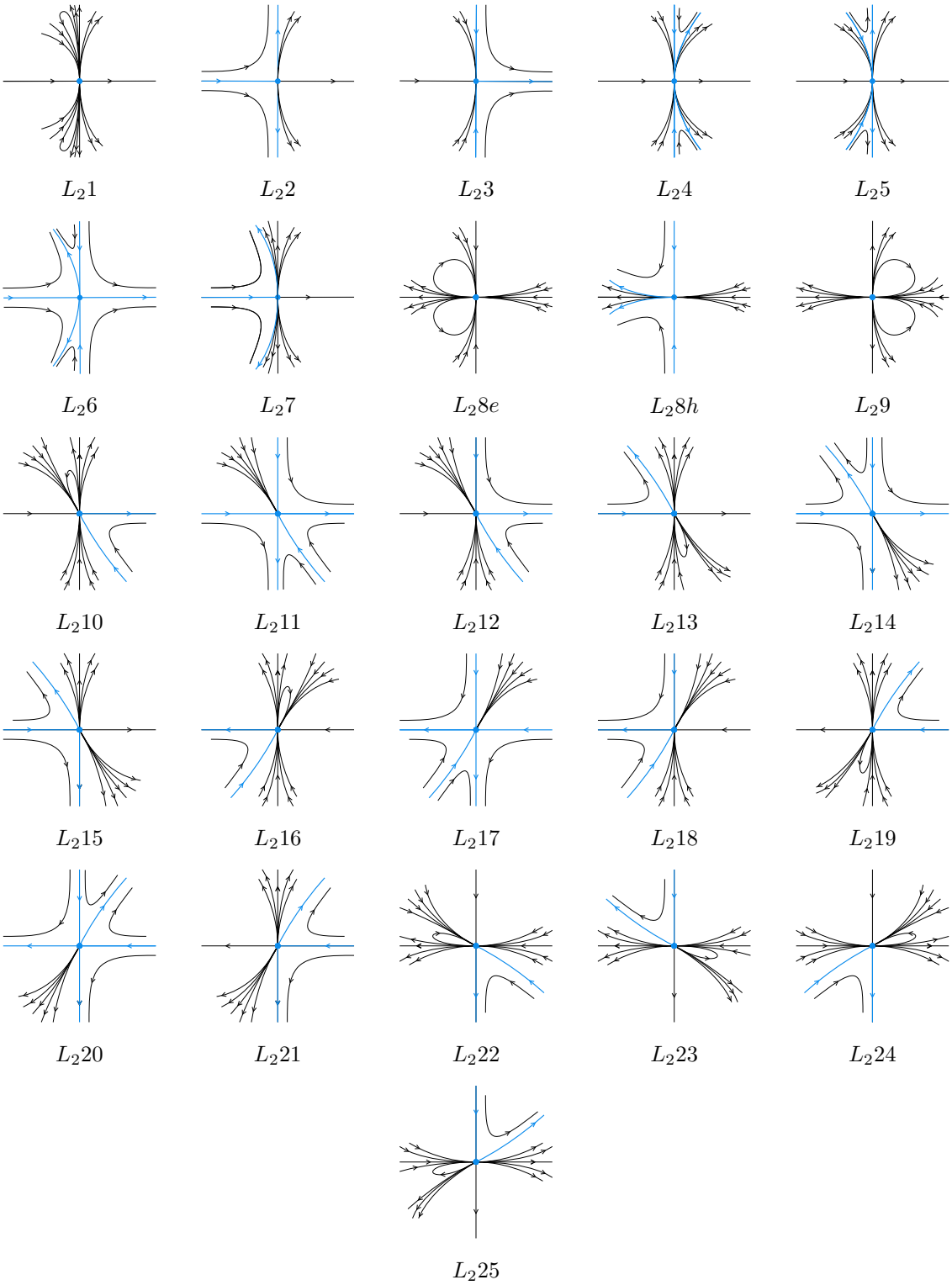

Figure 10: Local phase portraits of the infinite singular point O_2.

The singular points of systems (5.8) on the exceptional divisor are the origin Q_0 and the singular point $Q_1 = ((b_0 + c_0)/(b_1(\mu - 1)), 0)$ if $\mu \neq 1$ (note that it coincides with the origin if $b_0 + c_0 = 0$). We determine their local phase portraits obtaining the following classification. We start with the cases in which the only singular point on the exceptional divisor is the origin:

(a1) If $b_0 + c_0 = 0$ and $\mu \neq 1$, then the origin is a semi-hyperbolic saddle-node. If $\mu > 1$, it is necessary to do a vertical blow up of systems (6.3). We omit the details as the process is similar to the explained in case A1.1 for the singular point O_1. The phase portrait obtained for O_2 is given in Figure 2($L_2$1). If $\mu \in (-1, 1)$ we obtain phase portrait $L_2$2.

(a2) If $\mu = 1$ and $c_0(b_0 + c_0) > 0$, then the origin is a saddle. If $b_0 + c_0 < 0$ and $c_0 < 0$ we obtain again phase portrait $L_2$2 and if $b_0 + c_0 > 0$ and $c_0 > 0$ then we obtain phase portrait $L_2$3. In both cases it is necessary to do a vertical blow up of systems (6.3).

(a3) If $\mu = 1$, $c_0 < 0$, and $b_0 + c_0 > 0$, then the origin is an unstable node. We obtain phase portrait $L_2$1. Here the same consideration we made in case (a1) about the elliptic sectors applies. The blow ups do not determine if the elliptic sector appearing are indeed elliptic or hyperbolic, but this would be concluded analyzing the gobal phase portraits on Section 7. The same consideration applies also in (a7) when $\mu > 1$.

Now we consider the cases with two singular points on the exceptional divisor:

(a4) If $c_0 > 0$, $b_0 + c_0 > 0$ and $(b_0\mu + c_0)(\mu - 1) < 0$, then the origin is a saddle and Q_1 a stable node. From these conditions we can deduce that $\mu \in (-1, 1)$ and then we obtain only one phase portait which is the same $L_2$3.

(a5) If $c_0 < 0$, $b_0 + c_0 < 0$ and $(b_0\mu + c_0)(\mu - 1) > 0$, then Q_0 is a saddle and Q_1 is an unstable node. If $\mu > 1$ it is necessary to do a vertical blow up of systems (6.3), and then we obtain phase portrait $L_2$1. If $\mu \in (-1, 1)$ we obtain phase portrait $L_2$2.

(a6) If $c_0(b_0+c_0) > 0$ and $(b_0+c_0)(b_0\mu+c_0)(\mu-1) > 0$, then Q_0 and Q_1 are saddles. If $\mu \in (-1, 1)$, $b_0 + c_0 > 0$ and $c_0 > 0$ we easily obtain phase portrait $L_2$6. If $\mu > 1$, $b_0 + c_0 > 0$ and $c_0 > 0$ we obtain phase portrait $L_2$4 and if $\mu > 1$, $b_0 + c_0 < 0$ and $c_0 < 0$ we obtain phase portrait $L_2$5. In this two last cases it is necessary to do a vertical blow up of systems (6.3). We detail it for the first case, it is, with $\mu > 1$, $b_0 + c_0 > 0$ and $c_0 > 0$.

The phase portrait for (6.5) with the two saddles on the w_2-axis is given in Figure 11(a), and the corresponding for systems (6.4) is 11(b). If we undo the horizontal blow up, we must swap the third and fourth quadrants and shrink the w_2-axis into the origin. As a consequence the separatrices of the saddle Q_1 go into two separatrices with slope $(b_0+c_0)/(b_1(\mu-1))$, one of them goes to the origin in the third quadrant and the other leaves the origin in the first quadrant. There are four sectors, coloured in Figure 11(c), in which the behaviour is not determined, so we must do a vertical blow up.

Let introduce the variable $w_3 = v/w_1$ and eliminate a common factor w_1.We get the systems

$$\begin{aligned} \dot{w_1} &= b_2 w_1^2 w_3 + b_0 w_1 w_3 + b_1 w_1, \\ \dot{w_3} &= b_2(\mu - 1) w_1 w_3^2 - (b_0 + c_0) w_3^2 + b_1(\mu - 1) w_3. \end{aligned} \tag{6.6}$$

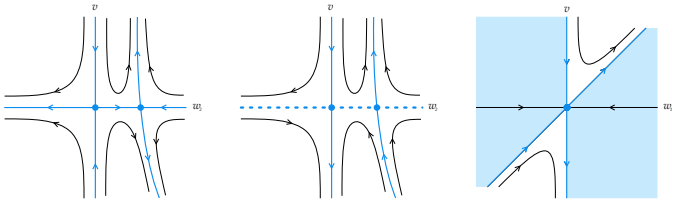

(a) (b) (c)

Figure 11: Desingularization of the origin of systems (6.1) case (a6) with $\mu > 1$, $c_0 > 0$ and $b_0 + c_0 > 0$.

These systems has two singular points on the exceptional divisor: the origin which is an unstable node, and the point $(0, b_1(\mu-1)/(b_0+c_0))$ which is a saddle. Studying the sense of the flow on the axes, we get that the phase portrait for systems (6.6) is the one in Figure 12(a). Multiplying by w_1 and undoing the vertical blow up, we obtain, respectively, the phase portraits on Figure 12(c) and (d). Now the phase portrait for systems (6.3) is well determined, and we just have to undo the first horizontal blow up, getting the final phase portrait $L_2 4$.

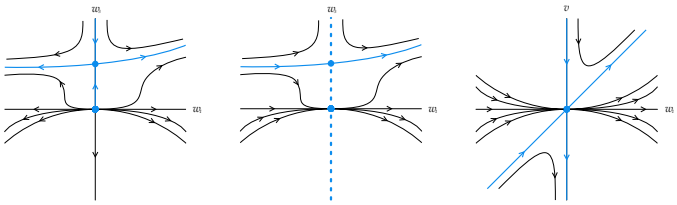

(a) (b) (c)

Figure 12: Desingularization of the origin of systems (6.1) case (a6) with $\mu > 1$, $c_0 > 0$ and $b_0 + c_0 > 0$.

(a7) If $c_0 < 0$, $b_0 + c_0 > 0$, and $(b_0\mu + c_0)(\mu - 1) > 0$, then Q_0 is an unstable node and $Q1$ is a saddle. If $\mu > 1$ we obtain phase portrait $L_2 1$ and if $\mu \in (-1, 1)$ we obtain phase portrait $L_2 7$.

(a8) If $c_0 < 0$, $b_0 + c_0 > 0$, and $(b_0\mu + c_0)(\mu - 1) < 0$, then Q_0 is an unstable node and $Q1$ is a stable node, and we obtain phase portrait $L_2 1$.

(b) If $b_3 = 0$, $c_0 \neq 0$ and $\mu < -1$ and $b_1 > 0$ then S_0 is a stable node. If $c_0 > 0$ we obtain phase portraits $L_2 8e$ and $L_2 8h$, which differ on the sectors that appear beside the v-axis on the second and third quadrants. On $L_2 8e$ we have elliptic sectors and on $L_2 8h$ we have hyperbolic sectors. We apply index theory on the global phase portraits to know which of them appears, see Section 7. If $c_0 < 0$ the result is similar and undetermined sector also appears when undoing the blow up. Nevertheless, in this case we have proved that in all the global phase portraits the undetermined sectors are elliptic, so then we have always phase portrait $L_2 9$.

(c) If $b_3 > 0$ and $\mu > -1$, then S_0 is a saddle and S_1 is a saddle-node. We distinguish four cases in function of the sign of b_1 which determines the position of S_1 and the sign of $b_0\mu + c_0$ which determines the position of the sectors of that singular point. With this signs fixed, we can determine and represent the phase portrait of systems (6.5) and (6.4). Then, in each of the four cases, when going back to the (u, v)-plane we must

distinguish three cases depending on wheter $\mu = 0$, $\mu \in (-1, 0)$ or $\mu > 0$. In the cases with $\mu > 0$ there appears an undefined sector which could be hyperbolic or elliptic. By doing an horizontal blow up in that cases, it can be determined that those sectors are always elliptic, but we omit the details as the process is the same that has been exposed in other cases. Another posibility is to prove directly on the global phase portrait, by applying index theory, that those sectors can only be elliptic. Now, to avoid repetitions, we simply include the results obtained in each case in the following table.

c1	$b_1 > 0$, $b_0\mu + c_1 > 0$	$\mu > 0$	$L_2 10$
		$\mu \in (-1, 0)$	$L_2 11$
		$\mu = 0$	$L_2 12$
c2	$b_1 > 0$, $b_0\mu + c_1 < 0$	$\mu > 0$	$L_2 13$
		$\mu \in (-1, 0)$	$L_2 14$
		$\mu = 0$	$L_2 15$
c3	$b_1 < 0$, $b_0\mu + c_1 > 0$	$\mu > 0$	$L_2 16$
		$\mu \in (-1, 0)$	$L_2 17$
		$\mu = 0$	$L_2 18$
c4	$b_1 > 0$, $b_0\mu + c_1 < 0$	$\mu > 0$	$L_2 19$
		$\mu \in (-1, 0)$	$L_2 20$
		$\mu = 0$	$L_2 21$

(d) If $b_3 > 0$, $\mu < -1$ and $b_1 > 0$, then S_0 is a stable node and S_1 is a saddle-node. The sign of $b_0\mu + c_0$ determines the position of the sectors of the saddle-node in systems (6.5) so we must distinguish two cases, and undo the blow up in each of them. If $b_0\mu + c_0 > 0$ we obtain phase portrait $L_2 23$ and if $b_0\mu + c_0 > 0$ we obtain $L_2 24$.

(e) If $b_3 > 0$, $\mu < -1$ and $b_1 < 0$, then S_0 is an unstable node and S_1 is a saddle-node. As in the previous case we distinguish the case with $b_0\mu + c_0 > 0$ in which we obtain phase portrait $L_2 25$ and the case with $b_0\mu + c_0 < 0$ in which we obtain phase portrait $L_2 26$.

7. Global phase portraits

In order to prove the global result stated in Theorem 0.1, we bring together the local information obtained in Sections 4, 5 and 6. We start our classification from the cases in Tables 2 to 5. In Table 6 we give, for each case of the Tables 2 to 5, the local phase portrait of the infinite singular points O_1 and O_2. In some of them the conditions determine only one local phase portrait in each one of the infinite singular points, but in most cases, we shall distinguish several possibilities depending on the parameters. Also in Table 6 we give the global phase portrait on the Poincaré disc obtained. All these global phase portraits are given in Figure 17, where we also indicate the number of separatrices (S) and canonical regions (R) that each of them has. We detail the reasonings in some cases, although they will not be showed in all of them to avoid repetitions. We recall that we are denoting the origins of charts U_1 and U_2 as O_1 and O_2 respectively, and in this section, to simplify the explanations, we will denote by Q_1 the origin of the chart V_1 and by Q_2 the origin of V_2.

7.1. Cases with a totally-determined local phase portrait at infinity

Case 1.3. Let consider the conditions $\mu < -1$ and $b_1 > 0$, so the infinite singular point O_1 has the local phase portrait $L_1 12$ given in Figure 2, and O_2 the phase portrait $L_2 23$ given in 10. We must combine the local information to get the global phase portait. The systems have an unstable node P_1 which is on the positive z-axis and a stable node P_2 which is on the negative x-axis. The origin is a saddle and it has the four separatrices over the axes (as the axes are invariant). Also, by the local configurations of O_1 and O_2 we know that the part of the z-axis which connects P_1 with O_1 is a separatrix and the part of the x-axis which connects P_2 with Q_1 is a separatrix. Appart from those, the systems have a separatrix leaving the singular point O_2 in the second quadrant and a separatrix which arrives at Q_1 on the third quadrant, see Figure 13. There is only one possible connection for these separatrices: the separatrix which leaves O_2 goes to P_2 and the separatrix which arrives at Q_1 starts at Q_2. Then we obtain phase portrait G9 in Figure 17, which has 19 separatrices and 6 canonical regions.

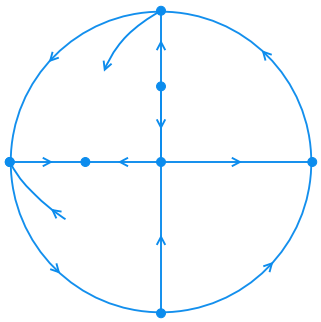

Figure 13: Separatrices provided by local information in case 1.3 with $\mu < -1$ and $b_1 > 0$.

With the same reasonings we can prove the other subcases in 1.3 and also the following: the subcases in 1.5 and 1.6 with $b_1 < 0$; all subcases in 1.8 and in 1.10; subcases in 2.2, 2.4 and 2.5 with $\mu < -1$; subcases in 3.2 with $\mu < -1$ or $\mu \in (-1, 0)$; subcases in 3.3, 3.4 and 3.5 with $\mu \in (-1, 0)$; subcases in 4.1 with $\mu < -1$ and subcases in 4.2 with $\mu \in (0, 1)$, $\mu = 1$ or $\mu > 1$.

7.2. Cases with undetermined sectors at infinity

Now we will deal with some cases in which the local phase portrait of O_1, O_2 or both was not totally determined in Sections 5 and 6, in the sense that they present certain sectors which can be either hyperbolic or elliptic.

Case 1.1 We consider $b_1 < 0$. The infinite singular point O_1 has the local phase portrait $L_1 13$ given in Figure 2, and O_2 the phase portrait $L_2 19$ given in Figure 10. We must prove here that the elliptic sectors on both phase portraits are indeed elliptic.

The systems have a saddle P_1 on the negative z-axis and a stable node P_2 on the negative x-axis. The origin is a saddle and it has the four separatrices over the axes. The repelling separatrices of P_1 are also over the z-axis, but the attracting ones should arrive to P_1, one in the third quadrant and other in the fourth quadrant. Also the systems have a separatrix leaving the singular point O_2 in the first quadrant and a separatrix leaving Q_1 on the second quadrant. Then, attending to the local phase portrait of each singular point, the only possible connection is the following: there is a separatrix which goes from Q_1 to

the point P_2 and a separatrix from O_2 to O_1, the attracting separatrix of P_1 on the third quadrant starts in Q_1 and the one in the fourth quadrant starts in Q_2. As a result, there is a canonical region delimited by Q_2, the part of the z-axis which connects this point with P_1, P_1, and its separatrix on the fourth quadrant, see Figure 14. If the sector on the local phase portrait of Q_2 were hyperbolic, then there would be any possible α or ω-limit on the boundary for the orbits in that region, but as it is not possible to have periodic orbits, this situation is no feasible, and this sector should be elliptic. The same happens with the elliptic sector at O_1. Anyway, this can be proved also anallitically by applying index theory.

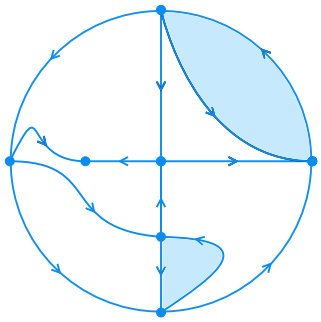

Figure 14: Separatrix configuration in case 1.1 with $b_1 < 0$ and regions in which local phase portrait was not determined.

By Theorem 1.2 the sum of the indices of all the singular points on the Poincaré sphere has to be 2. To compute this sum we must consider that the finite singular points on the Poincaré disc appear twice on the sphere (on the northern hemisphere and on the southern hemisphere). Thus if we denote by ind_F the sum of the indices of the finite singular points, and by ind_I the sum of the indices of the infinite singular points, the equality $2ind_F + ind_I = 2$ must be satisfied. In this particular case the finite singular points are two saddles whose index is -1, and a stable node which index is 1, so $ind_F = -1$. We deduce that ind_I must be 4. The infinite singular points are O_1 and Q_1 which have the same index, and O_2 and Q_2 which have also the same index.

The singular point O_1 has a hyperbolic sector so, if the non-determined sector is elliptic, from the Poincaré formula for the index given in Subsection 1.4, O_1 has index 1, and if the non-determined sector were hyperbolic, O_1 would have index 0. The same is valid for the singular point O_2. Then, if at any of these points O_1 or O_2 the sector were hyperbolic, the sum of the index of that point and its symmetric would be zero, and so the sum of the other point and its symmetric should be 4, which is not possible.

In other words,

$$ind_I = 2\left(\frac{E-H}{2}+1\right)+2\left(\frac{\tilde{E}-\tilde{H}}{2}-1\right),$$

where E and H are the number of elliptic and hyperbolic sectors of O_1 and $\tilde{E}$ and $\tilde{H}$ are the number of elliptic and hyperbolic sectors of O_2. As we know that $ind_I = 4$, then we obtain

$$(E+\tilde{E})-(H+\tilde{H})=0,$$

it is, considering both phase portraits of O_1 and O_2 together, there must be the same number of elliptic and hyperbolic sectors. As we have an hyperbolic sector in each of them, the two non-determined sectors must be elliptic.

Case 3.3 We consider $\mu < -1$. The infinite singular point O_1 has the local phase portrait $L_1 11$ given in Figure 2, and O_2 the phase portrait $L_2 8e$, but we must prove that we actually have $L_2 8e$ instead of $L_2 8h$.

The origin is an unstable node and the systems have a saddle P_2 on the negative x-axis. The attracting separatrices of P_2 are over the x-axis, but the repelling separatrices should leave P_2, one in the second quadrant and other in the third quadrant. There is also a separatrix leaving the singular point O_1 in the fourth quadrant. There is only one possible way to connect this separatices: the systems have a separatrix which goes from P_2 to O_2, another which goes from P_2 to Q_2 and the third one which goes from O_1 to Q_2. Then we have two canonical regions, the ones coloured in Figure 15, in which the only possibility is to have elliptic sectors whose orbits have as alpha and omega-limits the singular point O_2 and Q_2 respectively. We verify this with Theorem 1.2. As we have a finite saddle with index -1 and a finite node with index 1, then $ind_F = 0$. From the equality $2ind_F + ind_I = 2$ we know that ind_I must be 2.

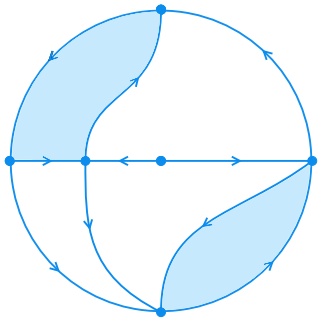

Figure 15: Separatrix configuration in case 3.3 with $\mu < -1$ and regions in which local phase portrait was not determined.

The local phase portrait of O_1 is well determined and it has four hyperbolic sectors and one parabolic sector, so

$$ind_{O_1} = \frac{E-H}{2} + 1 = \frac{0-4}{2} + 1 = -1,$$

and also we know that $ind_{O_1} = ind_{Q_1}$ and $ind_{O_2} = ind_{Q_2}$. Then

$$ind_I = 2ind_{O_1} + 2ind_{O_2} \Rightarrow ind_{O_2} = 2,$$

and by the Poincaré formula, if E and H are the number of elliptic and hyperbolic sector at O_2, then

$$\frac{E-H}{2} + 1 = 2 \Rightarrow E - H = 2,$$

and as we have only two sectors to determine wheter they are elliptic or hyperbolic, the only possibility is that both are elliptic.

With similar reasonings we can conclude and prove the results in all the remaining subcases, except the ones included in the following subsection.

7.3. Cases with three possible global phase portraits

Here we focus on the cases in which the separatrices can be connected in three different manners. As can be seen in Table 6 this happens in the subcases of 1.1, 1.2, 1.5, 1.6 and 1.7 in which $b_1 > 0$, in both subcases of 1.4, in the subcase of 1.9 with $b_1 < 0$ and in the subcase of 3.3 with $\mu = 0$, $b_3, b_1 > 0$. We give a detailed explanation in the following case:

Case 1.5. We consider the condition $\mu < -1$ and $b_1 > 0$. The origin is an unstable node, there is a stable node P_2 on the negative z-axis and saddle P_1 on the negative x-axis. The two attracting separatrices of P_1 are over the z-axis, and the repelling ones leave the origin in the third and fourth quadrants respectively. The infinite singular point O_1 has the local phase portrait $L_1 12$ of Figure 2, and O_2 the phase portrait $L_2 23$ of Figure 10. According to this local phase portraits, the positive z-axis, the positive x-axis, and the part of the negative x-axis between Q_1 and P_2 are separatrices. Moreover, there is another separatrix which leaves O_2 in the second quadrant and one that goes to Q_1 in the third quadrant. There is only one possible connection for the separatrices on the second and fourth quadrant, as it is represented in Figure 16(a).

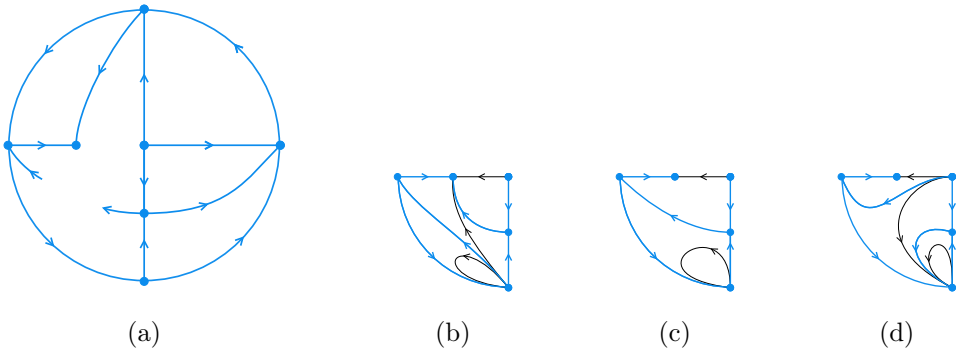

Figure 16: Separatrices and possible configurations on the third quadrant on case 1.5 with $\mu < -1$ and $b_1 > 0$.

We focus now on the third quadrant. We know that there is a separatrix leaving the point P_1 and another one going into Q_1. If we analyze the possible ω-limits of the separatrix leaving P_1 there are three options, the singular points Q_1, Q_2 and P_2. If the ω-limit is Q_1, then both separatrices should be the same, as the point Q_1 does not have parabolic sectors in the third quadrant. In that case, the configuration in the third quadrant is the one given in Figure 16 (c), and this leads to the global phase portrait G20.

If the ω-limit is P_2, then only possibility for the other separatrix is that its α-limit is Q_2. The configuration in the third quadrant is given in Figure 16(b), and this leads to the global phase portrait G19.

At last, if the ω-limit is Q_2, then the α-limit of the other separatrix is the origin. The configuration in the third quadrant is given in Figure 16(d), and this leads to the global phase portrait G21.

In phase portrait G20 we have proved that the connection of the separatrices takes place on the invariant straight line $z = -1/2$ for the values of the parameters $b_0 = b_2 = b_2 = c_0 = 1$, $b_1 = 2$ and $\mu = -2$. The two remaining phase portraits can be obtained by perturbing just one parameter.

We have also proved numerically, by using the program P4, see [13, Chapter 9], that the three global phase portraits are realizable.

In Table 7 we give the values of the parameters for which we have found each phase portrait, not only on this subcase but also in all the subcases in which three possibilities appear. In all of them we have check that the three possibilities are realizable and in all the triplets we have proved that in the phase portraits in which two separatrices connect, this connection takes place on an invariant straight line. More precisely, in the, phase portraits G2, G20, G24 and G45 the invariant line is $z = c_0/\mu b_3$ and in the phase portraits G6, G14, G28, G32, G36 and G81 the invariant line is $y = -b_0/b_2$.

Thus we have obtained the 106 global phase portaits given in Figure 17. There are 13 different classes according to their number of canonical regions and separatrices, and within each class we distinguish which ones are topologically equivalent in the following result.

Proposition 7.1. *For Kolmogorov systems* (0.3) *there are* 13 *classes according to the number of canonical regions and separatrices. Taking into account the topological equivalences, we get:*

(i) Seven distinct phase portraits with 7 canonical regions and 20 separatrices.

(ii) Six distinct phase portraits with 6 canonical regions and 19 separatrices.

(iii) Two distinct phase portraits with 8 canonical regions and 21 separatrices.

(iv) One phase portrait with 7 canonical regions and 21 separatrices.

(v) One phase portrait with 5 canonical regions and 18 separatrices.

(vi) Six distinct phase portraits with 7 canonical regions and 18 separatrices.

(vii) Eleven distinct phase portraits with 6 canonical regions and 17 separatrices.

(viii) Three distinct phase portraits with 5 canonical regions and 16 separatrices.

(ix) One phase portrait with 4 canonical regions and 15 separatrices.

(x) One phase portrait with 8 canonical regions and 19 separatrices.

(xi) Three distinct phase portraits with 5 canonical regions and 14 separatrices.

(xii) Six distinct phase portraits with 6 canonical regions and 15 separatrices.

(xiii) Four distinct phase portraits with 4 canonical regions and 13 separatrices.

Proof. We do the proof for every one of the thirtheen statements of the proposition.

(i) For systems (0.3) we have obtained 12 phase portaits with 7 canonical regions and 20 separatrices, namely, G1, G3, G4, G5, G7, G8, G14, G17, G19, G22, G31 and G33 of Figure 17. At first we divide the phase portraits in two subclasses attending to the index of the finite singular points.

In G1, G3, G4, G5, G7, G8, G14 and G17 the sum of the indices of the finite singular points is -1, and in the other phase portraits it is 1. Now we analyze the first subclass. G1 and G3 are topologically different because the boundary of the elliptic sectors in each of them is topologically different, by the same reason G1 is topologically different from G4 and G3 topologically different from G4. G1 is topologically equivalent to G5 by doing a symmetry with respect to the line $y - z = 0$ and a change of the time variable t by $-t$, and analogously G3 is topologically equivalent to G7 and G4 to G8. The phase portrait G14

is topologically different from G1 and G3 because in these two there are an elliptic sector with two finite singular points in the boundary which does not exist in G14. Also G14 is topologically different from G4 because the fourth quadrant of G14 is topologically different from all the quadrants of G4. This phase portrait G14 is topologically equivalent to G17 by a symmetry with respect to the line $y + z = 0$.

In the second subclass the phase portrait of G19 is topologically equivalent to G31 by a symmetry with respect to the line $y - z = 0$. The phase portrait of G19 is different from G22 and from G33, because the boundary of the elliptic sectors is different. G22 is topologically different from G33 because in the first one the saddle has two separatrices which connect to finite singular points and two separatrices which connect to infinite singular points, but in G33 there is only one separatrix which connects to a finite singular point.

Thus we have only 7 topologically distinct phase portraits between the 12 phase portaits with 7 canonical regions and 20 separatrices, which can be represented by G1, G3, G4, G14, G19, G22 and G33.

(ii) For systems (0.3) we have obtained 15 phase portaits with 6 canonical regions and 19 separatrices, namely, G2, G6, G9, G10, G11, G12, G20, G23, G25, G26, G27, G29, G30, G32 and G34 of Figure 17.

We can consider a first subclass with the phase portraits in which there are two elliptic sectors, i.e. G2 and G6, which are topologically equivalent by a symmetry with respect to the line $y - z = 0$ and by changing the time variable t by $-t$.

Consider now a second subclass with the phase portraits with only one elliptic sector which has in the boundary 2 singular points; this occurs in G9, G12, G26, G30 and G34. Here G9 is topologically equivalent to G12 by a symmetry with respect to the line $y - z = 0$ and a change of t by $-t$. G26 is the same as G12 if we move the saddle point to the origin, and G30 is the same as G26 with a symmetry along the line $y - z = 0$. At last, G30 and G34 are topologically different because the two singular points in the boundary of the elliptic sector in G30 are infinite and in G34 one is infinite and the other is finite.

In the remaining phase portraits there is only one elliptic sector and it has 3 singular points in the boundary. In the phase portraits G10, G11, G25 and G27 the saddle point has two separatrices which connect with infinite singular points. G10 is topologically equivalent to G11 by a symmetry along the line $y + z = 0$ and a change of t by $-t$; G10 is also topologically equivalent to G25 after moving the saddle of G25 to the origen, doing a rotation of -90º, a symmetry with respect to the z-axis and a change of t by $-t$. G25 is topologically equivalent to $G27$ with a symmetry along the line $y - z = 0$. In the phase portraits G20, G23, G29 and G32 the saddle point has three separatrices which connect with infinite singular points. Here G20 is topologically different from G23 because in both the position of the finite singular points is the same but the elliptic sector has a different position, so we can not get a transformation between them. By a symmetry with respect to the line $y - z = 0$ G23 is topologically equivalent to G29 and G20 topologically equivalent to G32.

Thus, we have 6 topologically different phase portraits between the 15 phase portaits with 6 canonical regions and 19 separatrices, which can be represented by G2, G9, G34, G10, G10 and G23.

(iii) We have obtained for systems (0.3) 4 phase portaits with 8 canonical regions and 21 separatrices, namely, G13, G15, G16 and G18 of Figure 17. By a symmetry with respect to the line $y + z = 0$ G13 is topologically equivalent to G16 and G15 topologically equivalent to G18. G13 is topologically different from G15 because the boundary of the elliptic sectors is different.

(iv) For systems (0.3) we have obtained only one phase portait with 7 canonical regions

and 21 separatrices, G21 of Figure 17.

(v) We have obtained for systems (0.3) 2 phase portaits with 5 canonical regions and 18 separatrices, G24 and G28 of Figure 17. These phase portraits are topologically equivalent by doing a symmetry with respect to the line $y - z = 0$.

(vi) We have obtained for systems (0.3) 14 phase portaits with 7 canonical regions and 18 separatrices, namely, G35, G37, G38, G43, G44, G46, G51, G56, G60, G68, G74, G80, G82 and G83 of Figure 17. We divide them inro three subclasses attending to the number of elliptic sectors that they have.

First, in G56, G60, G74, G80, G82 and G83 there is only one elliptic sector. G56 is topologically different from G60 because in the second one there is a finite singular point in the boundary of the elliptic sector, but in the first one there is not. We can transform G56 into G74 with a rotation of -90º and a change of t by $-t$; G60 into G80 with a symmetry with respect to the line $y - z = 0$; G80 into G83 with a symmetry with respect to the y-axis and G82 into G56 by moving the saddle point to the origin and doing a symmetry with respect to the line $y - z = 0$.

We consider now the subclass with two elliptic sectors, in which we have G35, G37, G38, G43, G44 and G46. Here G35 is topologically different from G37 and G38 because the boundary of the elliptic sectors is different. Also G37 is topologically different from G38, as in the last one there is a separatrix which connects two infinite singular points, and it does not exist in G37. We have that G35 and G44, G37 and G46, G38 and G43 these are topologically equivalent with a symmetry with respect to the line $y + z = 0$.

Finally, in G51 and G68 there are three elliptic sectors, and both are topologically equivalent by a symmetry with respect to the line $y - z = 0$ and changing t by $-t$.

Thus we have 6 topologically different phase portraits which can be represented by G56, G60, G35, G37, G38 and G51.

(vii) For systems (0.3) we have obtained 21 phase portaits with 6 canonical regions and 17 separatrices, namely, G36, G39, G40, G41, G42, G45, G47, G48, G49, G50, G55, G57, G61, G62, G70, G71, G75, G76, G77, G81 and G84 of Figure 17. We will divide them into four subclasses.

First, in G62 and G84 there are no elliptic sectors, and both phase portraits are symmetric with respect to the line $y - z = 0$.

Second, in G36 and G45 there are two elliptic sectors, and both are symmetric with respect to the line $y + z = 0$.

We consider now the phase portraits with one elliptic sector having the sum of the indices of the finite singular points equal to 1: G39, G40, G41, G42, G47, G48, G49 and G50. Due to the differences between the boundary of the elliptic sectors we get that G39 and G40, G39 and G41, G40 and G42, G41 and G42 are not topologically equivalent. Also G40 is not topologically equivalent to G41 because in G40 there are four separatrices which connect the origin with infinite singular points, but in G41 there are only three. Similarly, G39 is not topologically equivalent G42 because in G42 there are four separatrices which connect the finite saddle-node with infinite singular points, but in G39 there are only three. By doing a symmetry with respect to the line $y - z = 0$ we get that G41 and G47, G42 and G48, G39 and G49, G40 and G50 are topologically equivalent.

Finally we consider the phase portraits with one elliptic sector having the sum of the indices of the finite singular points equal to 0: G55, G57, G61, G70, G71, G75, G76, G77, G81. Again due to the differences between the boundary of the elliptic sectors we get that G55 and G57, G61 and G55, G61 and G57, G57 and G75, G61 and G75 are not topologically equivalent. G55 is topologically different from G75 because in G55 there are two separatrices

which connect infinite points but in G75 there are only one. G76 is topologically different from G57 and from G61 because in G76 there are two separatrices which connect infinite points, in G57 one and in G61 none. We can transform G55 into G70 and G57 into G71 with a simmetry with respect to the line $y - z = 0$ and a change of t for $-t$. If we rotate -90º the phase portrait G77 we obtain G61, and at last if we move the stable node of G75 to the origin, we do a symmetry with respect to the z-axis and we change t by $-t$ we obtain G81.

Thus we have 11 topologically different phase portraits between the 21 phase portaits with 6 canonical regions and 17 separatrices, that can be represented by G36, G39, G40, G41, G42, G55, G57, G61, G62, G75, G76.

(viii) For systems (0.3) we have obtained 8 phase portaits with 5 canonical regions and 16 separatrices.

In G52, G58, G72 and G79 there are two elliptic sectors, and these phase portraits are all topologically equivalent: if we move the node in G52 to the origin, we get G58; if we rotate 90º G52 we obtain G72, and with a symmetry with respect to the line $y - z = 0$ we transform G58 by G79.

In G54, G63, G73 and G85 there are only one elliptic sector. G54 and G63 are topologically different because the boundary of the elliptic sector is different. G54 becomes G73 with a rotation of 90º and G63 becomes G85 with a symmetry with respect to the line $y - z = 0$.

Thus we have three distinct phase portraits which can be represented by G52, G54 and G63.

(ix) For systems (0.3) we have obtained 2 phase portaits with 4 canonical regions and 15 separatrices, G53 and G69 of Figure 17. These phase portraits are topologically equivalent by doing a symmetry with respect to the line $y - z = 0$ and changing the time variable t by $-t$.

(x) For systems (0.3) we have obtained 2 phase portaits with 8 canonical regions and 19 separatrices, G59 and G78 of Figure 17. Both are topologically equivalent as we can obtain G78 if we do a rotation of 90º of G59.

(xi) For systems (0.3) we have obtained 5 phase portaits with 5 canonical regions and 14 separatrices, namely, G64, G66, G88, G89 and G100 of Figure 17. G66 has two elliptic sectors so it is topologically different from G64 and G100 which have only one. G64 is topologically different from G100 because the only finite singular point is the origin, which is a saddle-node in the first one and a saddle in the second one. With a symmetry with respect to the line $y - z = 0$ we transform G4 into G88, and G66 into G89. Thus we have 3 distinct phase portraits represented by G64, G66 and G100.

(xii) For systems (0.3) we have obtained 13 phase portaits with 6 canonical regions and 15 separatrices, namely, G65, G87, G90, G91, G93, G96, G97, G98, G99, G101, G102, G104 and G106 of Figure 17. We consider three subclasses depending on the number of the elliptic sectors.

In G65 G87, G90 and G91 there is only one elliptic sector. G65 is topologically equivalent to G87 with a rotation of 90º. G65 is topologically different from G90 because the boundary of the elliptic sectors is different, and by the same reason G95 is topologically different from G91, and G90 from G91.

In G93, G96, G97, G98 and G99 there are two elliptic sectors. G93 is topologically different from G96 because the boundary of the elliptic sectors is different. G93 is topologically equivalent to G98 with a symmetry with respect to the line $y + z = 0$ and a change of t by

$-t$; the same occurs with G96 and G99. Also G97 and G98 are symmetric with respect to the z-axis.

In G101, G102, G104 and G106 there are no elliptic sectors, and all these phase portraits are topologically equivalent. G101 is topologically equivalent to G102 moving the separatrix in the third quadrant to the negative z-axis. G102 is symmetric to G104 with respect to the line $y - z = 0$, and G104 is symmetric to G106 with respect to the z-axis.

In summary we have 6 topologically different phase portraits represented by G65, G90, G91, G93, G96 and G101.

(xiii) We have obtained for systems (0.3) 7 phase portaits with 4 canonical regions and 13 separatrices, namely, G67, G86, G92, G94, G95, G103 and G105 of Figure 17. If we rotate 90^{o} the phase portrait G67 we obtain G86. G67 is topologically different from G92 because they have different number of elliptic sectors. G92 is topologically equivalent to G94 with a symmetry with respect to the line $y + z = 0$ and a change of t by $-t$ and G94 topologically equivalent to G95 with a symmetry with respect to the z-axis. In G92 the only finite singular point is the origin, which is a saddle, and it is a node in G103, so both phase portraits are distinct. With the same argument G67 is topologically different from G103, G92 from G105, and G67 from G103. Finally G103 and G105 are topologically different because the first one has elliptic sectors but not the second one. Then we have 4 topologically different phase portraits represented by G67, G92, G103 and G105. □

The classification given in Table 6, proved in Subsections 7.1, 7.2 and 7.3, together with Proposition 7.1, prove our main result, i. e. Theorem 0.1 stated in Introduction.

Figure 1 includes the representatives of each one of the topological equivalence classes, which correspond to the portraits in Figure 17 as follows:

Rep.	**Phase portraits**
R1	G1, G5.
R2	G2, G6.
R3	G3, G7.
R4	G4, G8.
R5	G9, G12, G26, G30.
R6	G10, G11, G25, G27.
R7	G13, G16.
R8	G14, G17.
R9	G15, G18.
R10	G19, G31.
R11	G20, G32.
R12	G21.
R13	G22.
R14	G23, G29.
R15	G24, G28.
R16	G33.
R17	G34.
R18	G35, G44.

Rep.	**Phase portraits**
R19	G36, G45.
R20	G37, G46.
R21	G38, G43.
R22	G39, G49.
R23	G40, G50.
R24	G41, G47.
R25	G42, G48.
R26	G51, G68.
R27	G52, G58, G72, G79.
R28	G53, G69.
R29	G54, G73.
R30	G55, G70.
R31	G56, G74, G82.
R32	G57, G71.
R33	G69, G78.
R34	G60, G80, G83.
R35	G61, G77.
R36	G62, G84.

Rep.	**Phase portraits**
R37	G63, G85.
R38	G64, G88.
R39	G65, G87.
R40	G66, G89.
R41	G67, G86.
R42	G75, G81.
R43	G76.
R44	G90.
R45	G91.
R46	G92, G94, G95.
R47	G93, G97, G98.
R48	G96, G99.
R49	G100.
R50	G101, G102, G104, G106.
R51	G103.
R52	G105.

Case	Conditions	O_1	O_2	Global
1.1	$b_1 > 0$	$L_1 9$	$L_2 13$	G1, G2 or G3
	$b_1 < 0$	$L_1 13$	$L_2 19$	G4
1.2	$b_1 > 0$	$L_1 10$	$L_2 10$	G5, G6 or G7
	$b_1 < 0$	$L_1 14$	$L_2 16$	G8
1.3	$\mu < -1$, $b_1 > 0$	$L_1 12$	$L_2 23$	G9
	$\mu < -1$, $b_1 < 0$	$L_1 16$	$L_2 25$	G10
	$\mu \in (-1, 0)$, $b_1 > 0$	$L_1 18$	$L_2 14$	G11
	$\mu \in (-1, 0)$, $b_1 < 0$	$L_1 20$	$L_2 20$	G12
1.4	$b_1 > 0$	$L_1 10$	$L_2 10$	G13, G14 or G15
	$b_1 < 0$	$L_1 14$	$L_2 16$	G16, G17 or G18
1.5	$\mu < -1$, $b_1 > 0$	$L_1 12$	$L_2 23$	G19, G20 or G21
	$\mu < -1$, $b_1 < 0$	$L_1 16$	$L_2 25$	G22
	$\mu \in (-1, 0)$, $b_1 > 0$	$L_1 18$	$L_2 14$	G23, G24 or G25
	$\mu \in (-1, 0)$, $b_1 < 0$	$L_1 20$	$L_2 20$	G26
1.6	$\mu < -1$, $b_1 > 0$	$L_1 11$	$L_2 22$	G27, G28 or G29
	$\mu < -1$, $b_1 < 0$	$L_1 15$	$L_2 24$	G30
	$\mu \in (-1, 0)$, $b_1 > 0$	$L_1 17$	$L_2 11$	G31, G32 or G33
	$\mu \in (-1, 0)$, $b_1 < 0$	$L_1 19$	$L_2 17$	G34
1.7	$b_1 > 0$	$L_1 10$	$L_2 10$	G35, G36 or G37
	$b_1 < 0$	$L_1 14$	$L_2 16$	G38
1.8	$\mu < -1$, $b_1 > 0$	$L_1 12$	$L_2 23$	G39
	$\mu < -1$, $b_1 < 0$	$L_1 16$	$L_2 25$	G40
	$\mu \in (-1, 0)$, $b_1 > 0$	$L_1 18$	$L_2 14$	G41
	$\mu \in (-1, 0)$, $b_1 < 0$	$L_1 20$	$L_2 20$	G42
1.9	$b_1 > 0$	$L_1 10$	$L_2 10$	G43
	$b_1 < 0$	$L_1 14$	$L_2 16$	G44, G45 or G46
1.10	$\mu < -1$, $b_1 > 0$	$L_1 11$	$L_2 22$	G47
	$\mu < -1$, $b_1 < 0$	$L_1 15$	$L_2 24$	G48
	$\mu \in (-1, 0)$, $b_1 > 0$	$L_1 17$	$L_2 11$	G49
	$\mu \in (-1, 0)$, $b_1 < 0$	$L_1 19$	$L_2 17$	G50
2.1		$L_1 2$	$L_2 13$	G51
2.2	$\mu \in (-1, 0)$	$L_1 8e$	$L_2 14$	G52
	$b_0 + c_0 = 0$, $\mu > 1$	$L_1 1$	$L_2 10$	G53
	$b_0 + c_0 > 0$, $\mu \geq 1$.			
	$b_0 + c_0 \geq 0$, $\mu < -1$.	$L_1 3$	$L_2 23$	G54
	$b_0 + c_0 > 0$, $\mu \in (0, 1)$	$L_1 4$	$L_2 10$	G55
	$b_0 + c_0 < 0$, $\mu < -1$	$L_1 6$	$L_2 23$	G56
	$b_0 + c_0 < 0$, $\mu > 1$	$L_1 7$	$L_2 10$	G57
2.3	$\mu \in (-1, 0)$	$L_1 8e$	$L_2 14$	G58
	$\mu \in (0, 1)$	$L_1 4$	$L_2 10$	G59
	$\mu < -1$	$L_1 3$	$L_2 23$	G60
	$\mu \geq 1$	$L_1 1$	$L_2 10$	G61
2.4	$\mu \in (-1, 0)$	$L_1 8h$	$L_2 11$	G62
	$\mu < -1$	$L_1 5$	$L_2 22$	G63
2.5	$\mu \in (-1, 0)$	$L_1 8e$	$L_2 14$	G64
	$\mu \in (0, 1)$	$L_1 4$	$L_2 10$	G65
	$\mu < -1$	$L_1 3$	$L_2 23$	G66
	$\mu \geq 1$	$L_1 1$	$L_2 10$	G67

Case	Conditions	O_1	O_2	Global
3.1		$L_1 10$	$L_2 1$	G68
3.2	$b_0 + c_0 = 0,\ \mu > 0$	$L_1 9$	$L_2 2$	G69
	$b_0 + c_0 < 0,\ \mu \in (0, 1]$			
	$b_0 + c_0 < 0,\ \mu > 1$	$L_1 9$	$L_2 5$	G70
	$b_0 + c_0 < 0,\ \mu \in (0, 1)$	$L_1 9$	$L_2 7$	G71
	$\mu < -1$	$L_1 12$	$L_2 9$	G72
	$b_0 + c_0 \leq 0,\ \mu \in (-1, 0)$	$L_1 18$	$L_2 2$	G73
	$b_0 + c_0 \leq 0,\ \mu = 0,\ b_3 = 0$	$L_1 22eh$		
	$b_0 + c_0 > 0,\ \mu \in (-1, 0)$	$L_1 18$	$L_2 7$	G74
	$b_0 + c_0 > 0,\ \mu = 0,\ b_3 = 0$	$L_1 22eh$		
	$\mu = 0,\ b_3 > 0,\ b_1 > 0$	$L_1 22eh$	$L_2 15$	G75
	$\mu = 0,\ b_3 > 0,\ b_1 < 0$	$L_1 23eh$	$L_2 21$	G76
3.3	$\mu \in (0, 1]$	$L_1 10$	$L_2 3$	G77
	$\mu > 1$	$L_1 10$	$L_2 4$	G78
	$\mu < -1$	$L_1 11$	$L_2 8e$	G79
	$\mu \in (-1, 0)$	$L_1 17$	$L_2 3$	G80
	$\mu = 0,\ b_3 = 0$	$L_1 22he$		
	$\mu = 0,\ b_3 > 0,\ b_1 > 0$	$L_1 22he$	$L_2 12$	G80, G81 or G82
	$\mu = 0,\ b_3 > 0,\ b_1 < 0$	$L_1 23he$	$L_2 18$	G83
3.4	$\mu < -1$	$L_1 12$	$L_2 8h$	G84
	$\mu \in (-1, 0)$	$L_1 18$	$L_2 6$	G85
3.5	$\mu \in (0, 1]$	$L_1 10$	$L_2 3$	G86
	$\mu > 1$	$L_1 10$	$L_2 4$	G87
	$\mu < -1$	$L_1 11$	$L_2 8e$	G88
	$\mu \in (-1, 0)$	$L_1 17$	$L_2 3$	G89
	$\mu = 0,\ b_3 = 0$	$L_1 22he$		
	$\mu = 0,\ b_3 > 0,\ b_1 > 0$	$L_1 22he$	$L_2 12$	G90
	$\mu = 0,\ b_3 > 0,\ b_1 < 0$	$L_1 23he$	$L_2 18$	G91
4.1	$b_0 + c_0 \leq 0,\ \mu = 0,\ b_3 = 0$	$L_1 21e$	$L_2 2$	G92
	$b_0 + c_0 \leq 0,\ \mu \in (-1, 0)$	$L_1 8e$		
	$b_0 + c_0 = 0,\ \mu \in (0, 1)$	$L_1 2$		
	$b_0 + c_0 < 0,\ \mu \in (0, 1]$	$L_1 2$		
	$b_0 + c_0 > 0,\ \mu = 0,\ b_3 = 0$	$L_1 21e$	$L_2 7$	G93
	$b_0 + c_0 > 0,\ \mu \in (-1, 0)$	$L_1 8e$		
	$b_0 + c_0 > 0,\ \mu \in (0, 1),\ b_0\mu + c_0 < 0$	$L_1 2$		
	$b_0 + c_0 = 0,\ \mu > 1$	$L_1 1$	$L_2 1$	G94
	$b_0 + c_0 > 0,\ \mu \geq 1$			
	$b_0 + c_0 \geq 0,\ \mu < -1$	$L_1 3$	$L_2 9$	G95
	$b_0 + c_0 > 0,\ \mu \in (0, 1),\ b_0\mu + c_0 > 0$	$L_1 4$	$L_2 1$	G96
	$b_0 + c_0 < 0,\ \mu < -1$	$L_1 6$	$L_2 9$	G97
	$b_0 + c_0 < 0,\ \mu > 1,\ b_0\mu + c_0 > 0$	$L_1 7$	$L_2 1$	G98
	$b_0 + c_0 < 0,\ \mu > 1,\ b_0\mu + c_0 < 0$	$L_1 2$	$L_2 5$	G99
	$\mu = 0,\ b_3 > 0$	$L_1 21e$	$L_2 15$	G100
4.2	$\mu = 0,\ b_3 > 0$	$L_1 21h$	$L_2 12$	G101
	$\mu = 0,\ b_3 = 0$	$L_1 21h$	$L_2 3$	G102
	$\mu \in (-1, 0)$	$L_1 8h$		
	$\mu \in (0, 1)$	$L_1 4$		
	$\mu < -1,\ b_0\mu + c_0 > 0$	$L_1 5$	$L_2 8e$	G103
	$\mu < -1,\ b_0\mu + c_0 < 0$	$L_1 3$	$L_2 8h$	G104
	$\mu = 1$	$L_1 1$	$L_2 3$	G105
	$\mu > 1$	$L_1 1$	$L_2 4$	G106

Table 6: Classification of global phase portrais of systems (0.3).

Subcase	Phase portrait	Obtained for the values
1.1 $b_1 > 0$	G1	$b_0 = 1/2$, $b_1 = b_2 = b_3 = 1$, $c_0 = -1$, $\mu = 1/2$
	G2	$b_0 = 1/2$, $b_1 = b_2 = b_3 = 1$, $c_0 = -1$, $\mu = 1$
	G3	$b_0 = 1/2$, $b_1 = b_2 = b_3 = 1$, $c_0 = -1$, $\mu = 5/4$
1.2 $b_1 > 0$	G5	$b_0 = 2$, $b_1 = b_2 = b_3 = 1$, $c_0 = -1/2$, $\mu = 1$
	G6	$b_0 = b_1 = b_2 = b_3 = 1$, $c_0 = -1/2$, $\mu = 1$
	G7	$b_0 = 4/5$, $b_1 = b_2 = b_3 = 1$, $c_0 = -1/2$, $\mu = 1$
1.4 $b_1 > 0$	G13	$b_0 = 2$, $b_1 = b_2 = b_3 = c_0 = \mu = 1$
	G14	$b_0 = b_1 = b_2 = b_3 = c_0 = \mu = 1$
	G15	$b_0 = 1/2$, $b_1 = b_2 = b_3 = c_0 = \mu = 1$
1.4 $b_1 < 0$	G16	$b_0 = b_2 = b_3 = c_0 = \mu = 1$, $b_1 = -2$
	G17	$b_0 = 1$, $b_1 = -1$, $b_2 = b_3 = c_0 = \mu = 1$
	G18	$b_0 = b_2 = b_3 = c_0 = \mu = 1$, $b_1 = -1/2$
1.5 $\mu < -1$, $b_1 > 0$	G19	$b_0 = b_2 = b_3 = c_0 = 1$, $b_1 = 1$, $\mu = -2$
	G20	$b_0 = b_2 = b_3 = c_0 = 1$, $b_1 = 2$, $\mu = -2$
	G21	$b_0 = b_2 = b_3 = c_0 = 1$, $b_1 = 4$, $\mu = -2$
1.5 $\mu \in (-1, 0)$, $b_1 > 0$	G23	$b_0 = 4$, $b_1 = 1$, $b_2 = b_3 = c_0 = 1$, $\mu = -1/2$
	G24	$b_0 = 4$, $b_1 = 1/2$, $b_2 = b_3 = c_0 = 1$, $\mu = -1/2$
	G25	$b_0 = 4$, $b_1 = 1/10$, $b_2 = b_3 = c_0 = 1$, $\mu = -1/2$
1.6 $\mu < -1$, $b_1 > 0$	G27	$b_0 = 1/4$, $b_1 = b_2 = b_3 = 1$, $c_0 = 3$, $\mu = -2$
	G28	$b_0 = b_1 = b_2 = b_3 = 1$, $c_0 = 3$, $\mu = -2$
	G29	$b_0 = 5/4$, $b_1 = b_2 = b_3 = 1$, $c_0 = 3$, $\mu = -2$
1.6 $\mu \in (-1, 0)$, $b_1 > 0$	G31	$b_0 = b_1 = b_3 = 1$, $b_2 = 7/4$, $c_0 = 2$, $\mu = -1/2$
	G32	$b_0 = b_1 = b_2 = b_3 = 1$, $c_0 = 2$, $\mu = -1/2$
	G33	$b_0 = b_1 = b_3 = 1$, $b_2 = 1/4$, $c_0 = 2$, $\mu = -1/2$
1.7 $b_1 > 0$	G35	$b_0 = b_2 = b_3 = \mu = 1$, $b_1 = 7/8$, $c_0 = 0$
	G36	$b_0 = b_1 = b_2 = b_3 = \mu = 1$, $c_0 = 0$
	G37	$b_0 = b_2 = b_3 = \mu = 1$, $b_1 = 9/8$, $c_0 = 0$
1.9 $b_1 < 0$	G44	$b_0 = 0$, $b_1 = -1/2$, $b_2 = b_3 = c_0 = \mu = 1$
	G45	$b_0 = 0$, $b_1 = -1$, $b_2 = b_3 = c_0 = \mu = 1$
	G46	$b_0 = 0$, $b_1 = -2$, $b_2 = b_3 = c_0 = \mu = 1$
3.3 $\mu = 0$, $b_3 > 0$, $b_1 > 0$	G80	$b_0 = 2$, $b_1 = b_2 = b_3 = c_0 = 1$, $\mu = 0$
	G81	$b_0 = b_1 = b_2 = b_3 = c_0 = 1$, $\mu = 0$
	G82	$b_0 = 1/2$, $b_1 = b_2 = b_3 = c_0 = 1$, $\mu = 0$

Table 7: Values of the parameters for which each global phase portrait is obtained in cases with three possible configurations.

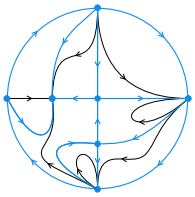

(G1) [R=7, S=20]

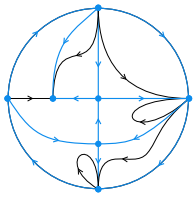

(G2) [R=6, S=19]

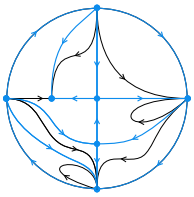

(G3) [R=7, S=20]

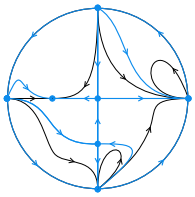

(G4) [R=7, S=20]

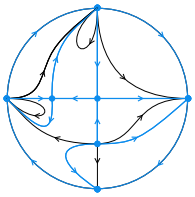

(G5) [R=7, S=20]

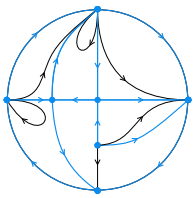

(G6) [R=6, S=19]

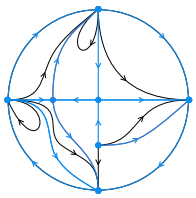

(G7) [R=7, S=20]

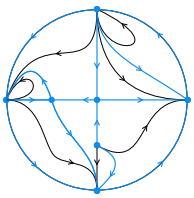

(G8) [R=7, S=20]

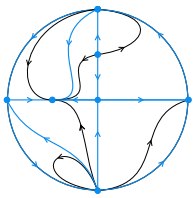

(G9) [R=6, S=19]

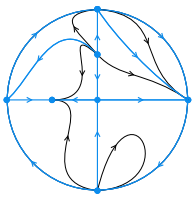

(G10) [R=6, S=19]

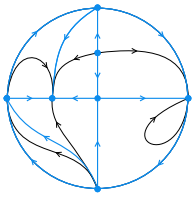

(G11) [R=6, S=19]

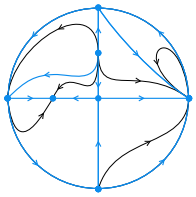

(G12) [R=6, S=19]

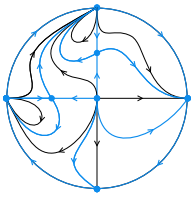

(G13) [R=8, S=21]

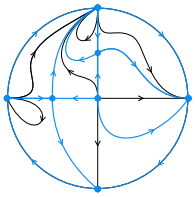

(G14) [R=7, S=20]

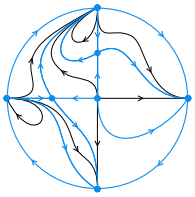

(G15) [R=8, S=21]

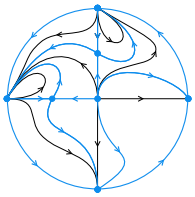

(G16) [R=8, S=21]

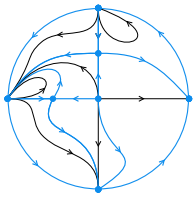

(G17) [R=7, S=20]

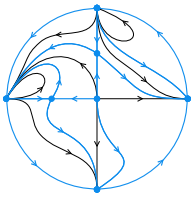

(G18) [R=8, S=21]

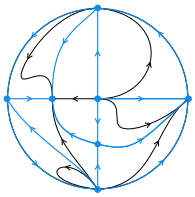

(G19) [R=7, S=20]

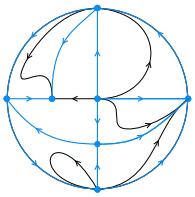

(G20) [R=6, S=19]

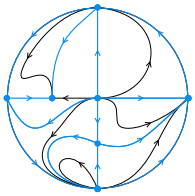

(G21) [R=7, S=21]

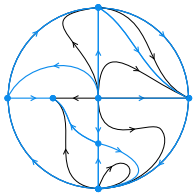

(G22) [R=7, S=20]

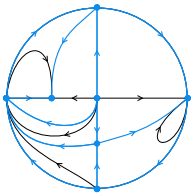

(G23) [R=6, S=19]

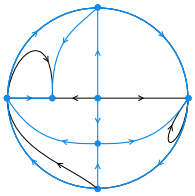

(G24) [R=5, S=18]

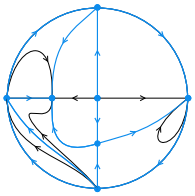

(G25) [R=6, S=19]

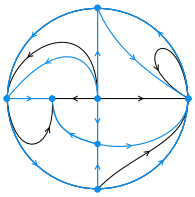

(G26) [R=6, S=19]

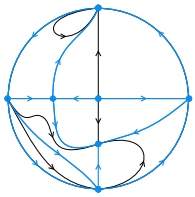

(G27) [R=6, S=19]

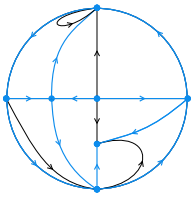

(G28) [R=5, S=18]

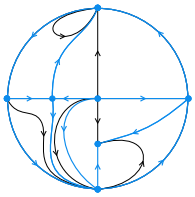

(G29) [R=6, S=19]

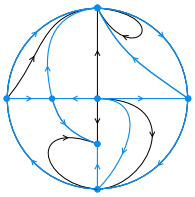

(G30) [R=6, S=19]

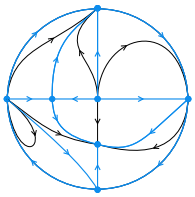

(G31) [R=7, S=20]

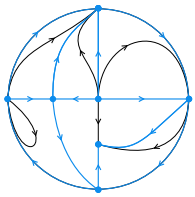

(G32) [R=6, S=19]

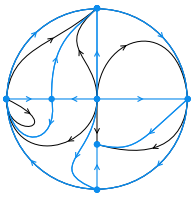

(G33) [R=7, S=20]

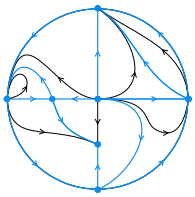

(G34) [R=6, S=19]

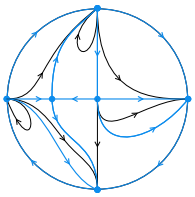

(G35) [R=7, S=18]

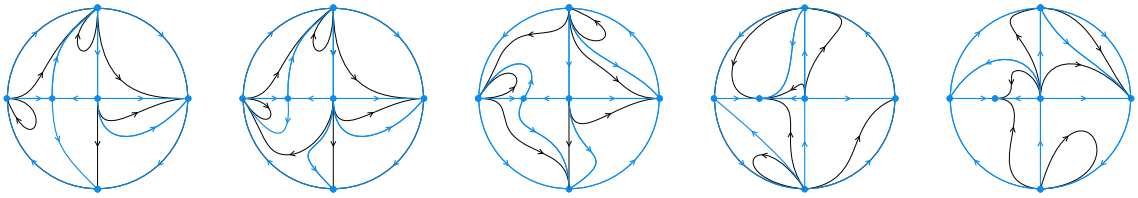

(G36) [R=6, S=17] (G37) [R=7, S=18] (G38) [R=7, S=18] (G39) [R=6, S=17] (G40) [R=6, S=17]

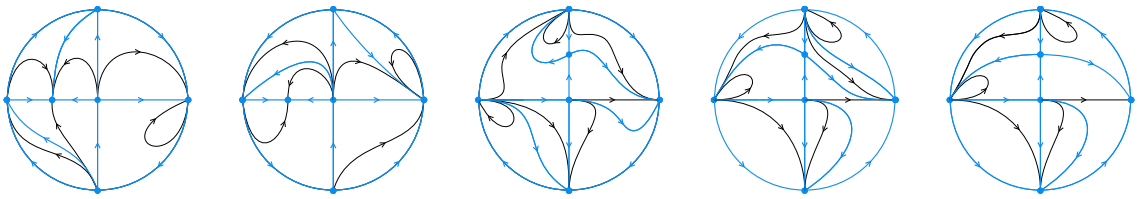

(G41) [R=6, S=17] (G42) [R=6, S=17] (G43) [R=7, S=18] (G44) [R=7, S=18] (G45) [R=6, S=17]

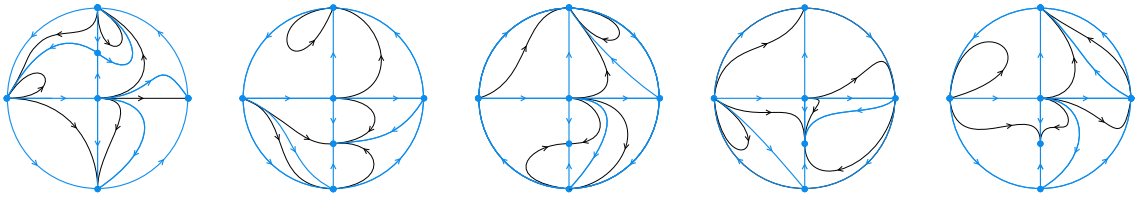

(G46) [R=7, S=18] (G47) [R=6, S=17] (G48) [R=6, S=17] (G49) [R=6, S=17] (G50) [R=6, S=17]

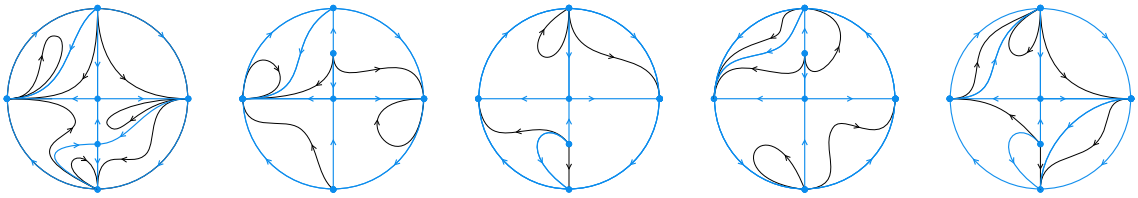

(G51) [R=7, S=18] (G52) [R=5, S=16] (G53) [R=4, S=15] (G54)[R=5, S=16] (G55) [R=6, S=17]

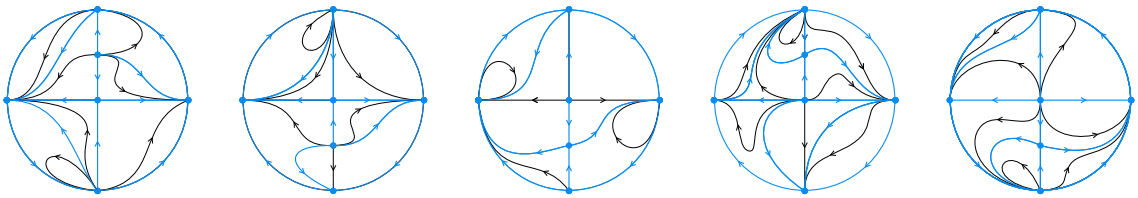

(G56) [R=7, S=18] (G57) [R=6, S=17] (G58) [R=5, S=16] (G59) [R=8, S=19] (G60) [R=7, S=18]

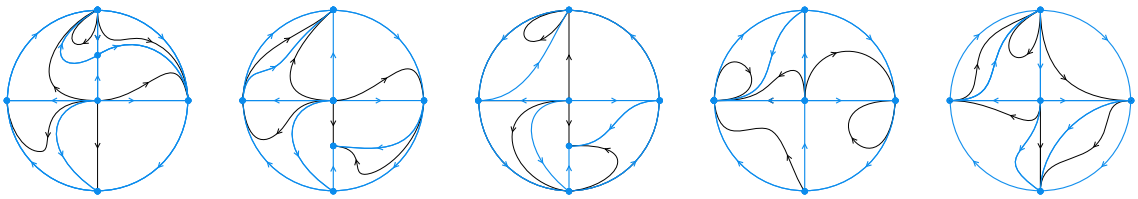

(G61) [R=6, S=17] (G62) [R=6, S=17] (G63) [R=5, S=16] (G64) [R=5, S=14] (G65) [R=6, S=15]

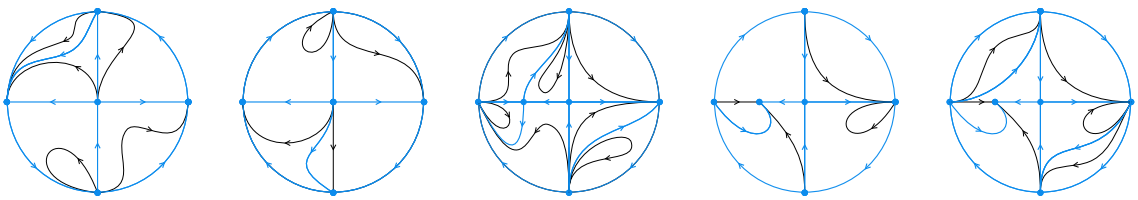

(G66) [R=5, S=14] (G67) [R=4, S=13] (G68) [R=7, S=18] (G69) [R=4, S=15] (G70) [R=6, S=17]

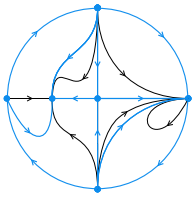
(G71) [R=6, S=17]
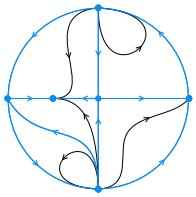
(G72) [R=5, S=16]
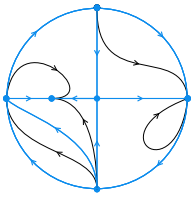
(G73) [R=5, S=16]
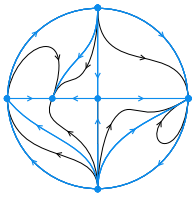
(G74) [R=7, S=18]
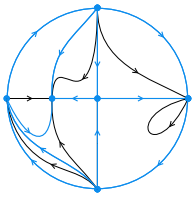
(G75) [R=6, S=17]

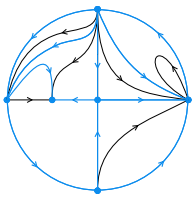
(G76) [R=6, S=17]
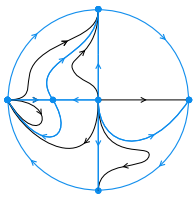
(G77) [R=6, S=17]
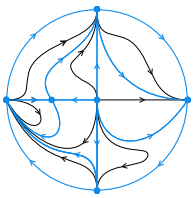
(G78) [R=8, S=19]
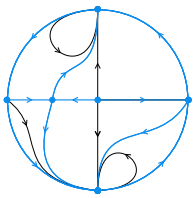
(G79) [R=5, S=16]
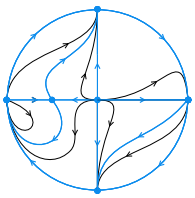
(G80) [R=7, S=18]

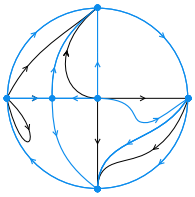
(G81) [R=6, S=17]
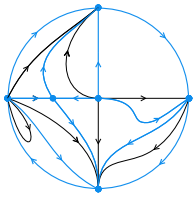
(G82) [R=7, S=18]
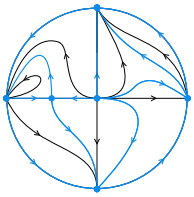
(G83) [R=7, S=18]
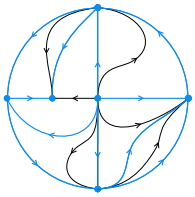
(G84) [R=6, S=17]
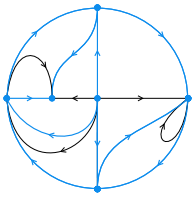
(G85) [R=5, S=16]

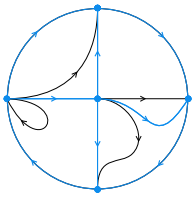
(G86) [R=4, S=13]
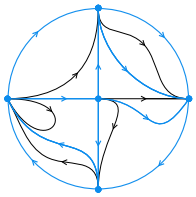
(G87) [R=6, S=15]
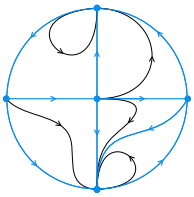
(G88) [R=5, S=14]
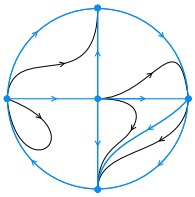
(G89) [R=5, S=14]
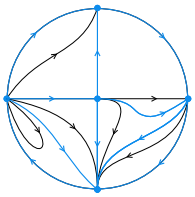
(G90) [R=6, S=15]

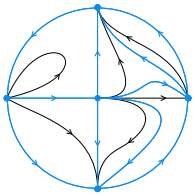
(G91) [R=6, S=15]
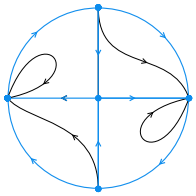
(G92) [R=4, S=13]
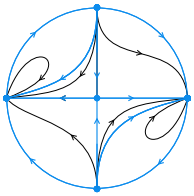
(G93) [R=6, S=15]
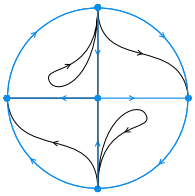
(G94) [R=4, S=13]
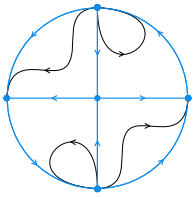
(G95) [R=4, S=13]

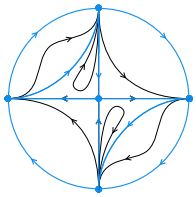
(G96) [R=6, S=15]
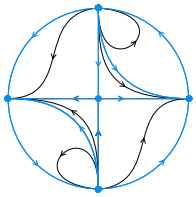
(G97) [R=6, S=15]
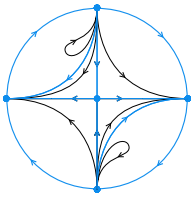
(G98) [R=6, S=15]
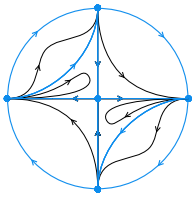
(G99) [R=6, S=15]
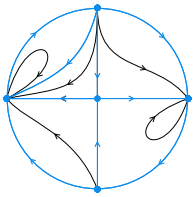
(G100) [R=5, S=14]

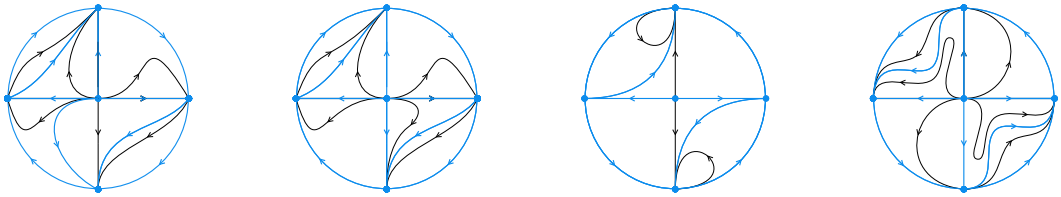

(G101) [R=6, S=15] (G102) [R=6, S=15] (G103) [R=4, S=13] (G104) [R=6, S=15]

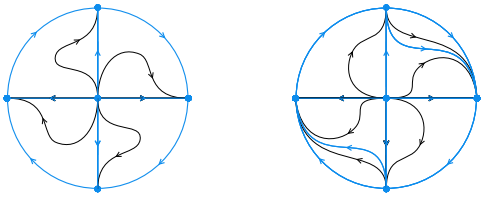

(G105) [R=4, S=13] (G106) [R=6, S=15]

Figure 17: Global phase portraits of systems (0.3) in the Poincaré disc.

8. Acknowledgments

The authors would like to thank the reviewers for their valuable suggestions that that have allowed us to improve the presentation of our paper.

The first and third authors are partially supported by the Ministerio de Economía, Industria y Competitividad, Agencia Estatal de Investigación (Spain), grant MTM2016-79661-P (European FEDER support included, UE) and the Consellería de Educación, Universidade e Formación Profesional (Xunta de Galicia), grant ED431C 2019/10 with FEDER funds. The first author is also supported by the Ministerio de Educacion, Cultura y Deporte de España, contract FPU17/02125.

The second author is partially supported by the Ministerio de Ciencia, Innovación y Universidades, Agencia Estatal de Investigación grant PID2019-104658GB-100 (FEDER), the Agència de Gestió d'Ajuts Universitaris i de Recerca grant 2017SGR1617, and the H2020 European Research Council grant MSCA-RISE-2017-777911.

Bibliography

[1] Alavez-Ramírez, J., Blé, G., Castellanos V. & Llibre, J. [2012] "On the global flow of a 3-dimensional Lotka–Volterra system," *Nonlinear Anal.-Theor.* **75**, 4114–4125.

[2] Álvarez, M. J., Ferragut, A. & Jarque, X. [2011] "A survey on the blow up technique," *Int. J. Bifurcat. Chaos* **21**, 3103–3118.

[3] Andronov, A. A., Leontovich, E. A., Gordon, I.J. & Maier, A. G. [1973] *Qualitative Theory of Second Order Dynamic Systems*, (J. Wiley & Sons).

[4] Arneodo, A., Coullet, P., Tresser, C., [1980] "Occurrence of strange attractors in three-dimensional Volterra equations," *Phys. Lett.* **79A**, 259–263.

[5] Arneodo, A., Coullet, P., Peyraud, J. et al., [1982] "Strange attractors in volterra equations for species in competition," *J. Math. Biology* **14**, 153–157.

[6] Artés, J. C., Dumortier, F., Herssens, C., Llibre, J. & De Maesschalck, P. [2005] "Computer program P4 to study phase portraits of planar polynomial differential equations." http://mat.uab.es/ artes/p4/p4.htm.

[7] Breitenlohner, P., Lavrelashvili, G. & Maison, D. [1998] "Mass inflation and chaotic behaviour inside hairy black holes," *Nucl. Phys. B* **524**, 427–443.

[8] Busse, F. H. [1981] "Transition to turbulence via the statistical limit cycle route," *Haken H. (eds) Chaos and Order in Nature. Springer Series in Synergetics* **11**, Springer-Verlag, Berlin.

[9] Coste, J., Peyraud, J., & Coullet, P. [1979] "Asymptotic behaviors in the dynamics of competing species," *SIAM J. App. Math.* **36**, 516–543.

[10] Desai, M. & Ormerod, P. "Richard Goodwin: A short appreciation" *Econ. J.* **108**, 1431–1435.

[11] Diz-Pita, E., Llibre, J. & Otero-Espinar, M. V. [2021] "Phase portraits of a family of Kolmogorov systems depending on six parameters," *Electron. J. Differ. Eq.* **2021**, 1–38.

[12] Dumortier, F. [1977] "Singularities of vector fields on the plane," *J. Differ. Equations* **23**, 53–106.

[13] Dumortier, F., Llibre J. & Artés, J.C. [2006] *Qualitative theory of planar differential systems*, (UniversiText, Springer-Verlag, New York).

[14] Fu, X., Zhang, P. & Zhang, J. [2017] "Forecasting and analyzing internet users of China with Lotka-Volterra model", *Asia-Pac J. Oper. Res.* **34**.

[15] Gandolfo, G. [2009] *Economic dynamics*, Fourth edition, (Springer, Heidelberg).

[16] Gandolfo, G. [2008] "Giuseppe Palomba and the Lotka–Volterra equations," *Rend. Lince. - Sci. Fis.* **19**, , 347–357.

[17] Goodwin, R. M. [1967] "A Growth Cycle", *Essays in economic dynamics. Palgrave Macmillan*, (Cambridge University Press, London).

[18] Hering, R. [1990] "Oscillations in Lotka-Volterra systems of chemical reactions," *J. Math. Chem.* **5**, 197–202.

[19] Kolmogorov, A. [1936] "Sulla teoria di Volterra della lotta per l'esistenza" *Gi. Inst. Ital. Attuari* **7**, 74–80.

[20] Laval, G. & Pellat, R. [1975] "Plasma Physics", *Proceedings of Summer School of Theoretical Physics* (Gordon and Breach, New York).

[21] Llibre, J. & Martínez, Y. [2020] "Dynamics of a competitive Lotka-Volterra system in $\mathbb{R}^3$, " *Acta Appl. Math.* **170**, 569–577.

[22] Llibre, J. & Xiao, D. M. [2014] "Global dynamics of a Lotka-Volterra model with two predators competing for one prey," *SIAM K. Appl. Math.* **74**, 434–453.

[23] Llibre, J. & Zhang, X. [2009] "Darboux theory of integrability for polynomial vector fields in $\mathbb{R}^n$ taking into account the multiplicity at infinity," *B. Sci. Math.*, 765–778.

[24] Llibre, J. & Zhang, X. [2009] "Darboux theory of integrability in $\mathbb{C}^n$ taking into account the multiplicity," *J. of Differ. Equations*, 541–551.

[25] Llibre, J. & Zhang, X. [2010] "Rational first integrals in the Darboux theory of integrability in $\mathbb{C}^n$," *B. Sci. Math.* **2010**, 189–195.

[26] May, R. M. [1974] *Stability and complexity in model ecosystems*, (Princeton NJ).

[27] Markus, L. [1954] "Global structure of ordinary differential equations in the plane," *Trans. Amer. Math. Soc.* **76**, 127–148.

[28] Neumann, D.A. [1975] "Classification of continuous flows on 2-manifolds," *Proc. Amer. Math. Soc.* **48**, 73–81.

[29] Peixoto, M. M. [1973] *Proccedings of a simposium held at the university of Bahia*, (Acad. Press, New York,) 349–420.

[30] Schlomiuk, D. & Vulpe, N. [2012] "Global topological classification of Lotka–Volterra quadratic differential systems," *Electron. J. Differ. Eq.*

[31] Smale, S.,[1976] "On the differential equations of species in competition," *J. Math. Biology* **3**, 5–7.

[32] Wijeratne, A. W., Yi, F. & Wei, J. [2009] "Bifurcation analysis in the diffusive Lotka–Volterra system: an application to market economy," *Chaos Soliton. Fract.* **40**, 902–911.